An Roinn Comhshaoil,
Aeráide agus Cumarsáide
Department of the Environment,
Climate and Communications

The Climate Action Regional Offices are an initiative of the Government of Ireland funded by the department of the Environment, Climate and Communications and managed through Local Authorities.

Urban Heat Island in County Dublin

An examination of its temporal and spatial properties and causes



Oifig Réigiúnach um
Ghníomhú ar son na hAeráide
Rialtas Áitiúil
Réigiún Cathrach Bhaile Átha Cliath

Climate Action
Regional Offices
Local Government
Dublin Metropolitan

CARO

Acknowledgement

This report builds upon the original Urban Heat Island (UHI) report prepared for Dublin City Council under the BUILD-CAPACITIES Project. The current report extends the assessment to include all four local authorities within the Dublin region.

The authors would like to thank Benjamin Bechtel and Jonas Kittner, who extracted temperature data from Netatmo sensors in Dublin that were shared by CWS owners. The authors also acknowledge the World Urban Database and Access Portal Tools (WUDAPT) (Ching et al., 2018) contributors for making the global LCZ map (Demure et al., 2022) possible through their contribution of training areas to the LCZ Generator (demure et al., 2021). The authors would also like to acknowledge the support and guidance provided by the Dublin Metropolitan Climate Action Regional Office (DM CARO).

The authors wish to acknowledge the Research IT HPC Service at University College Dublin for providing computational facilities and support that contributed to the research results reported in this report.

Authors
Dr Ankur Prabhat Sati and Prof Gerald Mills
School of Geography, University College of Dublin, Ireland

Executive Summary

Urban areas typically experience higher air and surface temperatures when compared to surrounding non-urban (rural) regions, a phenomenon known as the Urban Heat Island (UHI) effect. This difference in temperature results from aspects of form and functions of the cities. Form refers to the physical characteristics of the urban landscape, which includes building dimensions and layout (geometry), construction materials (fabric) and surface cover (vegetation/paving). These properties modify the natural exchanges of energy at the surface, shifting more of the available energy to heat storage and direct heating of the overlying atmosphere and reducing evaporative cooling. Urban functions refer to human activities and resources needed to sustain these, which results in anthropogenic heat emissions. As cities grow and the climate warms, understanding and mitigating UHI effects becomes vital for urban resilience, energy planning, and public health.

There are several types of urban heat island (UHI) but the most studied are the canopy-level and surface UHIs. The latter refers to higher temperatures at the ground and surfaces of buildings (walls and roofs) in cities, when compared to natural surfaces outside the city. The canopy UHI refers to the near surface air temperature, which represents the temperatures the people feel at street level. The focus of this report is on the canopy-layer UHI; a complementary report will focus on the surface UHI using observations from thermal imagery from satellite platforms. This canopy-layer UHI is assessed using a network of crowdsourced weather stations (CWS), official meteorological data, and advanced numerical modelling. The research aims to better understand the temporal and spatial dynamics of the urban thermal effect in Dublin. It has two objectives:

1. To assess the spatial and temporal characteristics of the canopy-level UHI using observations and modelling, and map UHI intensity across Dublin county, and
2. To evaluate the implications for climate resilience and energy policy, especially in the context of climate change.

Methodology Overview: This report uses temperature observations made at CWS across Dublin to describe the UHI effect and combines these with simulations generated by a climate model to understand the processes responsible for temperature variations. We use the statistics of the UHI to assess its impact on building energy use, in the context of global climate change.

Observation on the UHI utilise a CWS network created from over 200 privately-owned weather stations distributed across Dublin, each of which publishes their data online. Following data quality controls, 120 stations with temporal coverage from 2020–2023 are included in this analysis. These stations are distributed across the urban landscape, which is heterogenous. Here we use Local Climate Zones (LCZ) to distinguish between types of urban neighbourhoods and categorise the CWSs into areas with same characteristics (e.g., city centre, midtown, suburbs and industrial areas). Temperature observations are compared to data at three Met Eireann meteorological stations: Dublin Airport (DAP), Casement Aerodrome, and Phoenix Park (PHP). The analysis focused on hourly and seasonal temperature trends, identifying UHI intensities through comparisons between suburban stations and rural reference points. These data are used to compile a climatology of Dublin's UHI. High-resolution simulations of Dublin's UHI were conducted using the Weather Research and Forecasting (WRF) model, which can account for the urban effect. This model is run for selected weather conditions when the UHI effect is strongest. Additionally, we explore the surface UHI based on MODIS and ECOSTRESS-3 satellites during 2020.

Urban heat island statistics were used to calculate heating (HDD) and cooling (CDD) degree days which can be used to assess impacts on building energy use for heating and cooling respectively.

Key Findings:

- Urban Heat Island Characteristics: Dublin experiences pronounced UHI effects, particularly during summer nights, with average nocturnal intensities of up to 4.3 °C and peaks exceeding 5.5 °C in dense city centre and industrial zones. UHI typically forms after sunset, peaks around midnight, and collapses at sunrise.
- Spatial Distribution and Temporal Variability: Maps of UHI intensity reveal that the highest temperature anomalies are in the city centre and industrial estates, while parks and coastal zones exhibit cooler conditions (so-called "cold pools"). Temporal analysis shows that the canopy-level UHI peaks several hours after sunset and decreases thereafter, disappearing completely near sunrise as surface warming and boundary layer mixing occurs.
- Crowdsourced Weather Stations (CWS) Validation: While data from CWS instruments has quality issues (associated with non-standard placement and sporadic availability), the data can provide reliable temperature observations, if quality checks are performed. Comparison with official data showed strong alignment, particularly in identifying temperature patterns and UHI cycles. These results underscore the feasibility of using CWS networks for urban climate monitoring.
- Local Climate Zones (LCZs): These describe a scheme for categorising urban neighbourhoods into universal types for the purpose of UHI analysis. Cities can be mapped into LCZ types and used to examine thermal effects. Here, the analysis demonstrated the role of urban morphology in influencing thermal behaviour. Densely built zones exhibited higher nocturnal UHI, while open low-rise and green suburban areas cooled faster and had significantly lower UHI intensities. Industrial zones also displayed elevated nighttime UHI due to retained and generated heat.
- Degree Days and Energy Implications: The study calculated Cooling Degree Days (CDD) and Heating Degree Days (HDD) across the city. In a typical year, there are no CDDs recorded at Dublin Airport (DAP), but residential areas indicated growing CDDs. In comparison, HDDs at DAP were consistently higher than that recorded in residential areas of the city. Met Éireann now produces data for building design, based on Dublin Airport. These results suggest a need for refined zone-specific energy management policies. Replace reliance on airport observations with urban-resolved monitoring to inform building energy codes, resilience planning, and public health measures.
- Climate Change Projections: Using projections from Nolan (2024), the study estimates that by 2071–2100, under a high emissions scenario, CDD values in high-density urban area (LCZ2) could increase by over 30 days annually. Concurrently, HDD are projected to decrease by more than 200 days. These shifts reinforce the importance of adapting building energy strategies and urban planning to emerging climate realities.

Conclusions and Policy Recommendations: The research demonstrates the value citizen weather station (CWS) data for urban climate studies when quality assurance protocols are applied. Crowdsourced weather data can significantly enhance the spatial resolution of urban climate monitoring, bridging gaps left by sparse official networks.

The study confirms that Dublin experiences significant UHI intensities, which vary across the urbanised landscape. These intensities are greatest at night, during calm conditions, and under clear skies in summer. Urban design, material use, and green infrastructure are key factors influencing these patterns. Furthermore, degree day analysis highlights discrepancies between observed and policy-assumed energy demand, underlining the importance of using urban-resolved metrics in planning.

Future climate projections indicate that Dublin will experience higher cooling demands and reduced heating needs, emphasizing the need for city-specific integration of climate resilience and energy efficiency policies. The 2020–2023 UHI analysis shows that central and midtown areas remain significantly warmer at night than surrounding suburbs, underscoring the urgency for targeted adaptation. Key measures include expanding green infrastructure such as parks, trees, and green roofs

and improving building design and retrofitting to reduce indoor overheating and enhance urban sustainability. The findings support a coordinated policy approach centred on four key areas:

- enhancing monitoring and modelling capacity by expanding Dublin's meteorological network for more accurate, spatially resolved data.
- Integrate "Heat Zoning" into Planning to promote climate-sensitive design and expand green and blue infrastructure.
- strengthening climate adaptation and public health measures through an Urban Heat Action Plan, improved building standards, and targeted support for vulnerable populations and outdoor workers.
- refining energy and climate policies by using localized temperature data to improve energy efficiency and promote passive cooling systems.

Collectively, these actions aim to reduce heat exposure, enhance urban resilience, and improve overall liveability under a warming climate.

1 Introduction

Urban Heat Islands (UHI) occur in cities around the world, where urbanisation leads to higher temperatures compared to surrounding rural areas. In this report we investigate county Dublin's UHI using observations and modelling and assess its impact on building energy use. There are few official weather stations in the Dublin area (and none are in the city centre) so we rely on temperature observations from citizen weather stations (CWS), which transmit data to the internet We focus on the period since 2020 when the CWS data is available and select case-study period to examine the formation of the UHI in detail; we focussed on the weather conditions likely to maximise the intensity of the UHI. Finally, the role of urban landcover and land use is explored using the Local Climate Zones (LCZ) typology which was developed for UHI studies and represents an international typology of urban neighbourhood characteristics. The model used is the Weather Research Forecasting (WRF) model which includes urban processes.

The outline structure of report is as follows:

1. Introduction

The introduction sets the context of the Urban Heat Island (UHI) effect, explaining its forms and relevance for Dublin. It reviews past UHI research, the opportunities and limitations of crowdsourced weather data, and the value of numerical models such as WRF for analysing urban climates.

2. Data and Methodology

This section presents Dublin as the study area, describing its geography, climate, and available meteorological stations. It introduces the citizen-based Netatmo weather station network, organised into Local Climate Zones (LCZ), and explains the data processing and quality control steps that refined the network into a robust dataset for UHI analysis.

3. UHI Climatology

In this section, hourly and seasonal temperature patterns between 2020 and 2023 are analysed. The results show distinct diurnal cycles across suburban and reference sites, with UHI intensity peaking after sunset in summer and dissipating at sunrise.

4. Summertime UHI

Focusing on the period from June to August, this section examines anticyclonic weather conditions (fair weather days) that enhance UHI development. It compares diurnal cycles across LCZs, showing strongest intensities in built-up areas and industrial areas, and demonstrates slower cooling in urban areas. Simulated UHI patterns are then presented for selected anticyclonic days, demonstrating the timing, spatial structure, and genesis of UHI across the city. The canopy layer UHI analysis is complemented by daytime surface UHI derived from ECOSTRESS and night-time surface UHI from the MODIS Aqua product.

5. Implications of UHI and Policy recommendations

The implications of UHI are assessed through Cooling Degree Days (CDD) and Heating Degree Days (HDD). Results show higher cooling needs in residential zones and reduced heating demand compared with airport data, raising concerns about the suitability of using airport observations for policy. Climate projections indicate increasing CDD and decreasing HDD, underscoring shifts in future energy demand.

6. Conclusions

The report concludes that crowdsourced data, once quality-controlled, are reliable for urban climate analysis. Dublin's UHI is shown to vary with form, weather type, and time of day, with green spaces playing a key mitigating role. The findings highlight implications for planning, energy management, and climate resilience under future warming. This section presents policy recommendations derived from UHI indicators. These guidelines aim to support strategies for mitigating urban heat impacts.

1.1 The Urban Heat Island

The urban heat island (UHI) describes the thermal effect of urbanisation. The two commonly studied UHI types (Figure 1) are:

- The surface UHI (SUHI), which refers to the urban effect on temperature on the ground, walls and roofs. It is generally measured using thermal cameras that record the temperature of the visible surface from remote platforms, such as drones, aircraft and satellites.
- The canopy-level UHI (CUHI)

Land Surface Temperature (LST) based SUHI analysis complements canopy layer UHI by capturing different but interrelated aspects of urban thermal environments. LST reflects the radiative temperature of surfaces such as roads, roofs, and vegetation, providing high spatial detail on how land cover, materials, and urban morphology influence heat storage and release. In contrast, canopy layer UHI represents air temperature within the urban canopy, which is more directly relevant to human exposure and thermal comfort. While canopy temperatures integrate atmospheric processes such as mixing, advection, and shading, LST highlights the underlying surface drivers of these processes. Together, they offer a more complete understanding of urban heat dynamics: LST helps identify hotspots and surface-based mitigation opportunities (e.g., greening, albedo changes), while canopy layer UHI captures the realised thermal environment experienced by people. Urban Heat Islands (UHIs) form due to differences in the absorption and emissivity of various surface types. For instance, water bodies warm up more slowly than urban materials but also cool down more gradually. Similarly, open land, forests, and built-up areas have distinct land surface and canopy layer temperatures depending on how much sunlight they reflect and absorb. (Figure 1)

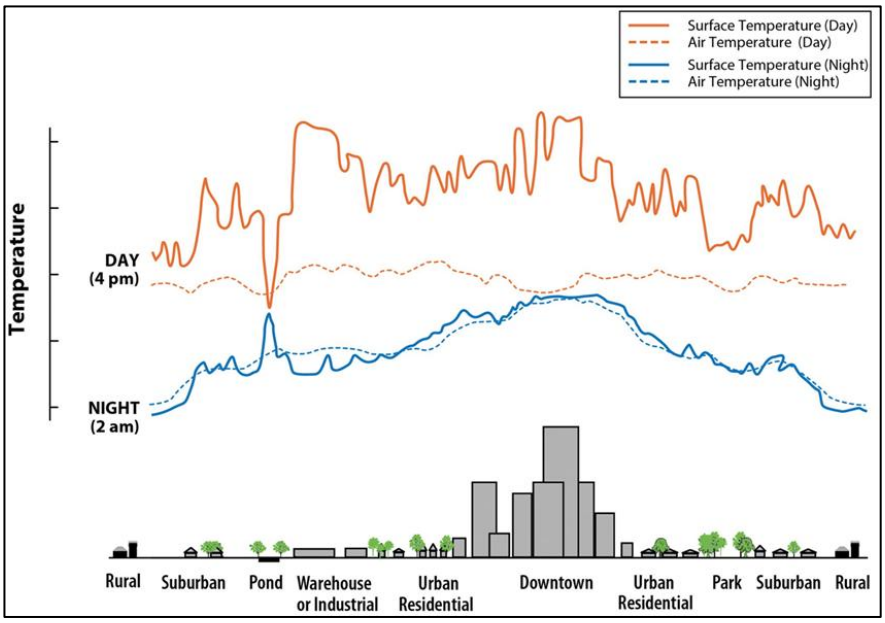

Figure 1: The differences in surface and canopy layer temperatures for different landscapes based on their absorption and emissivity

The real time example of these differences in the land surface temperatures is reflected in the summertime peak temperatures across Dublin for the summers of 2013-2022. It is seen in figure 2 that the waterbodies (Irish sea) tend to be cooler than the built-up area during the daytime. Similarly, the densely built-up areas, suburbs and the vegetated areas show huge differences in the peak temperatures during summertime. Phoenix Park and St Anne's Park act as cool oases, with temperatures typically 5–6 °C lower than surrounding areas, while smaller parks such as St Stephen's Green and Merrion Square are still noticeably cooler, by about 2–3 °C. The Dublin Mountains in the south also show lower temperatures owing to their altitude.

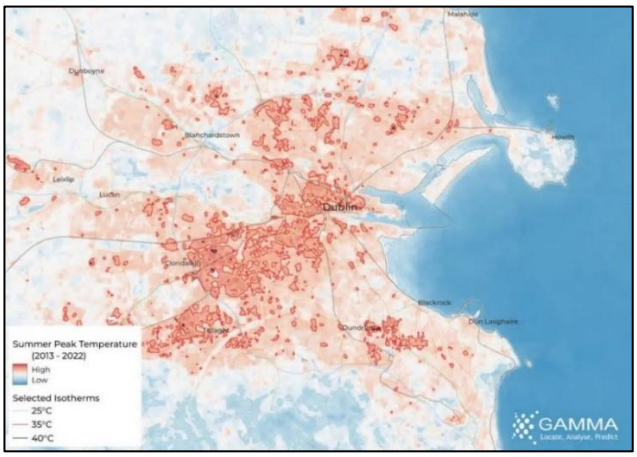

Figure 2: Dublin Summer Peak Temperature (2013 – 2022)

The near-surface air temperature (the canopy-level UHI, CUHI) is the focus of this work and is defined by the air temperature difference (ΔT) between observations made natural/rural (r) and over urban (u) landscapes, that is ΔTu-r. In this framework, the near-surface temperature over a rural surface represents the 'natural' environment in the absence of the city (Figure 3) and ΔTu-r represents the urban thermal effect. The magnitude of the CUHI depends on the character of both the rural and urban landscapes and the weather conditions and varies over space and time.

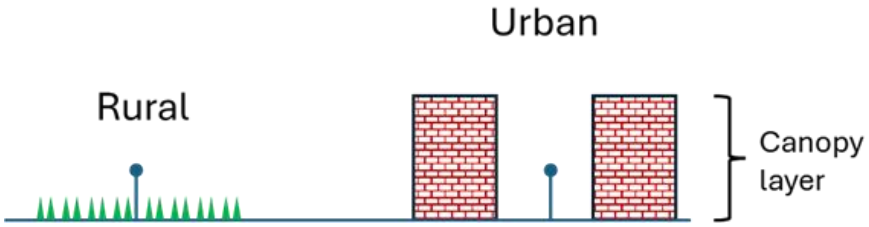

Figure 3: A simple diagram showing a station located over a rural (grass) surface and over a street, within the urban canopy layer.

The evidence from a great many studies shows that the UHI increases in magnitude from the suburbs to the city centre (Figure 2) and is correlated with increased impermeable surface cover and higher built density. UHI studies also show that the canopy-level UHI is essentially a night-time phenomenon as the urban landscape cools slower than the rural environment, such that ΔTu-r is greatest several hours after sunset. The weather circumstances that maximize this cooling effect are associated with calm conditions, clear skies following a dry period.

There is not a single standard method to study the CUHI (Stewart, 2011) but two common approaches are the use of weather stations at fixed locations and/or mobile stations (Alexander and Mills, 2014). The use of fixed stations provides detailed temporal information that can be used to generate a climatology of the CUHI but the spatial information is limited by the number of stations and their distribution across

the city (Figure 2). By comparison, transects[1] can provide spatial on the variations of the CUHI in different parts of the city but is limited by the number of transects that can be completed so that limited temporal information is obtainable. As a result, fixed stations are often used to plot the temporal development of the CUHI under different weather conditions and mobile transects are used to examine spatial patterns under selected weather conditions. Ideally, we need a network of weather stations in the city and outside to capture the temporal and spatial statistics of the CUHI.

Professional monitoring networks carefully select representative urban sites and employ high-quality instruments alongside modern communication systems to deliver reliable, high-quality data. In the case of Dublin, such data are essential for developing a detailed understanding of the Urban Heat Island (UHI) effect, enabling robust analysis of its spatial patterns, intensity, and underlying drivers. Muller et al. (2013) conducted a systematic overview of urban meteorological networks; well-known examples are the Birmingham Urban Climate Laboratory (Chapman et al., 2015, Warren et al., 2016), the Oklahoma City Micronet (Basara et al., 2011) and the Helsinki testbed (Koskinen et al., 2011). An alternative approach is to 'create' an urban network using private-owned (amateur) weather stations. There are several websites that acquire and publish the observations of citizen weather stations (CWS) online and, for many cities, there are enough stations that could support an analysis of the UHI; however, these stations do not adhere to conventional weather station standards and the data quality need to be quality assessed. Nevertheless, these CWS networks can provide high-resolution data cost-effectively.

The causes of the UHI can be framed in the context of the surface energy budget (as energy units Watts per squared meter, Wm^{-2}), which states that net radiation (Q^*) is channelled into heating the substrate (ΔQ_S), and turbulent exchanges of sensible (Q_H) and latent (Q_E) with the near-surface atmosphere:

$$Q^* + Q_F = Q_H + Q_E + \Delta Q_S$$

The additional term here (Q_F) is the anthropogenic heat contribution (urban functions). Each of these terms is changed in cities (Table 1).

Table 1: The urban effect on energy exchanges.

Term	Urban Effect
Net Radiation (Q^*)	Radiation exchanges are affected by building layout which 'traps' radiation within the canopy layer; this effect restricts access to the sky and inhibits night-time cooling
Anthropogenic heat exchange (Q_F)	Human activities result in heat emissions from vehicles and buildings.
Turbulent sensible heat exchange (Q_H)	This is the dominant (non-radiant) exchange between the surface and adjacent atmosphere.
Turbulent latent heat exchange (Q_E)	The lack of vegetation means that Q_E is small in dense urban areas.
Substrate heat exchange (ΔQ_S)	Urban materials are dense and can store heat effectively during the day and loses heat slowly at night,

[1] A transect is a line or path across an area along which observations or measurements are taken at regular intervals to study spatial variation.

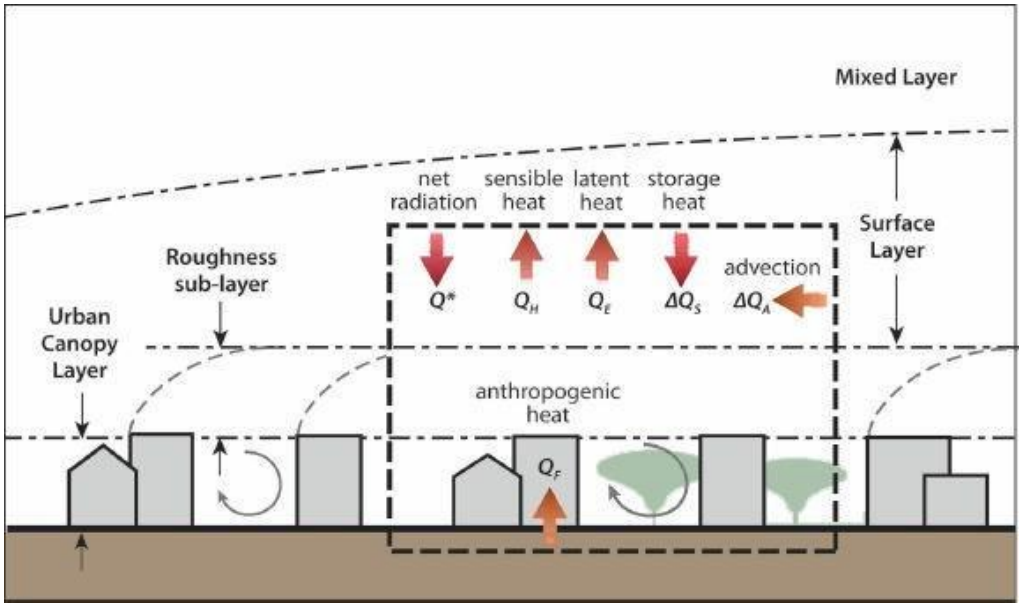

Figure 4: Schematic section showing urban surface energy balance components. Arrows pointing inwards represent energy gains to the system, and arrows pointing outwards represent energy loss from the system (Source: After Erell et all, Urban Microclimate, 2011)

Under clear, dry and calm weather conditions (typically associated with anticyclones) the difference between urban and rural environments is accentuated. During the daytime the urban environment absorbs solar radiation, much of which is stored in the substrate.

The elevated mean temperature of urban settings associated with the UHI phenomenon has significant impacts on urban living conditions. Two of the most frequently discussed impacts of the UHI are health risks (e.g: Laaidi et al., 2012; Levermore et al., 2017) and the energy demand of buildings (e.g.: Santamouris, 2014; Kolokotorni et al., 2012). Dublin faces growing risks from extreme heat events. Although Ireland's temperate climate has historically limited the impact of heat waves, climate change is expected to increase both the frequency and intensity of hot periods. UHI effect further amplifies risks within Dublin, where built-up areas retain heat, exposing vulnerable populations to sustained high nighttime temperatures. Studies of historical data from 1981–2003 show that heat waves in Ireland, though infrequent, have been linked with observable excess mortality (Pascal 2011). In Dublin, mortality risks were more pronounced among the elderly and those with pre-existing cardiovascular and respiratory conditions. While overall excess deaths during heat waves were higher in rural areas, urban centres like Dublin suffer additional stress due to UHI effects, which increase exposure to prolonged heat.

Although the UHI effect on building energy use is well recognized, its quantitative impacts remain understudied. Most research focused on typical buildings using urban and rural temperature data in physics-based models, while few explored spatial (intra- and inter-city) variations. Within cities, UHI impacts were greatest in urban centres and declined toward rural areas, mirroring UHI intensity patterns (Li et al., 2019). Adopting sustainable energy policies and practices offers cities and governments key strategies to mitigate urban heat islands. This analysis by Anser et al., (2025) provides insights for emerging economies on managing the complex relationship between UHIs and energy dynamic where they indicated that in China, urban energy use may decline by 2030 through energy efficiency initiatives. However, cooling energy demand is not a significant concern in Dublin because its climate is characterized by cool conditions and relatively cold winters, which create a persistent need for space heating. In Dublin, total energy consumption may vary under UHI effects, as reduced heating demand could be offset by a slight increase in cooling energy use.

This report provides a comprehensive framework for understanding UHI dynamics through a synergistic approach combining citizen science, climatological analysis, and advanced numerical modelling. The insights are directly relevant for urban planners, policymakers, health experts, energy providers, and researchers aiming to adapt to a warming urban future.

2. Data and Methodology

2.1 Study region

Dublin County, located on the east coast of Ireland, covers an area of approximately 922 km^2 and had a population of 1,501,500 at the 2022 Census. It is the most populous county in the country and forms the core of the Greater Dublin Area. Administratively, the county is divided into four local authority (LA) areas: Dublin City, Fingal, South Dublin, and Dún Laoghaire-Rathdown. Population density varies considerably across the county, with highly dense urban cores, particularly within Dublin City transitioning to lower-density suburban and peri-urban areas toward the outskirts. The built environment reflects this gradient, comprising historic 18th and 19th-century architecture in central areas, extensive mid-to-late 20th-century suburban development, and more recent housing estates, commercial zones, and industrial areas distributed along major transport corridors.

Synoptic meteorological stations with length range of data recordings are operating in three locations: at the Dublin Airport, at the Casement Aerodrome and in the Phoenix Park (Figure 5). The recording of meteorological parameters at these units follows the WMO guidelines and the details of the various parameters recorded at these three stations are provided in Appendix A.

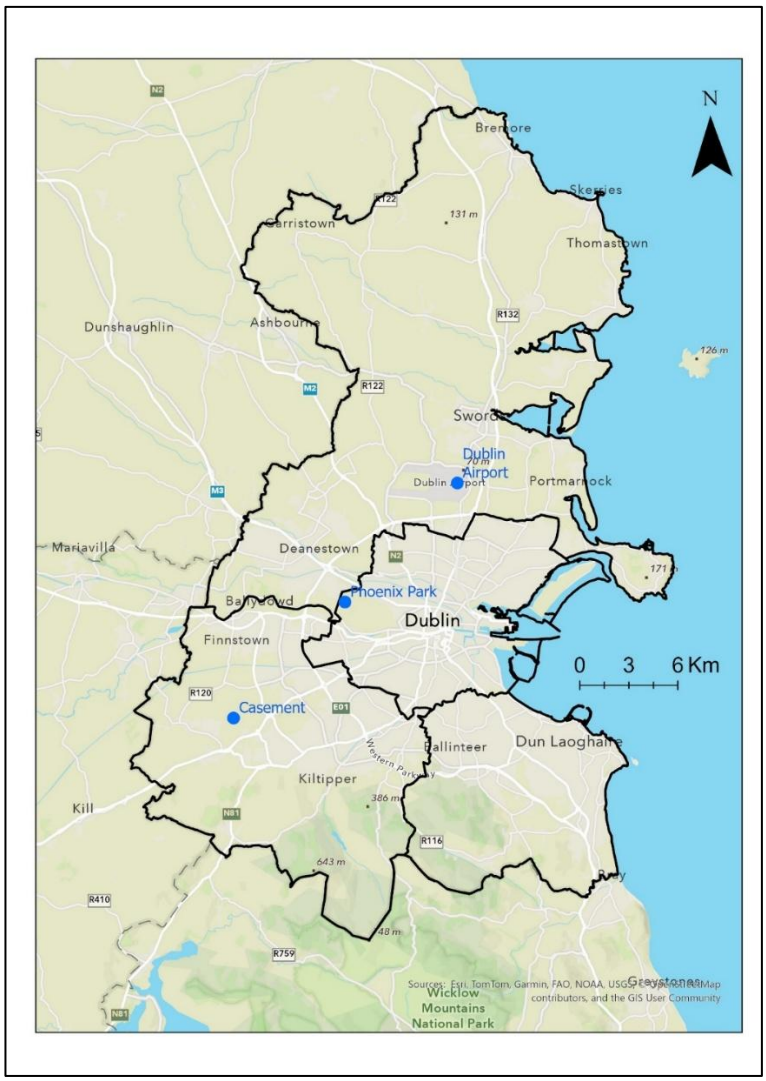

Figure 5: The study region (Dublin county) and location of three met stations within Dublin.

The climate of Dublin is classified as Koppen type temperate oceanic (Cfb) with mild winters, cool summers and consistent rainfall throughout the year. Weather variations are mostly associated with the passage of mid-latitude frontal cyclones (MLC). Dublin's fortunate topography provides a natural shelter from the prevailing southerly and south-westerly winds and the rainfall associated with the weather fronts from these directions and makes the city one of the warmest and driest place in the country. The lowest monthly mean air temperatures are around 5.0˚ in January, while the highest are in July around 15˚C. The low-lying parts of the city only receive 600 to 800mm precipitation annually and even the wettest parts of the town, the mountainous S-SW of Dublin only experiences around 1000mm of rainfall per annum. Humidity remains consistent high year-round, averaging 73–83%, with winter peaks in December–January (≈83–96%) and a slight decline in spring (April–June, ≈68–80%). This persistent moisture, driven by frequent rainfall and proximity to the sea, often makes conditions feel damp even when temperatures are mild.

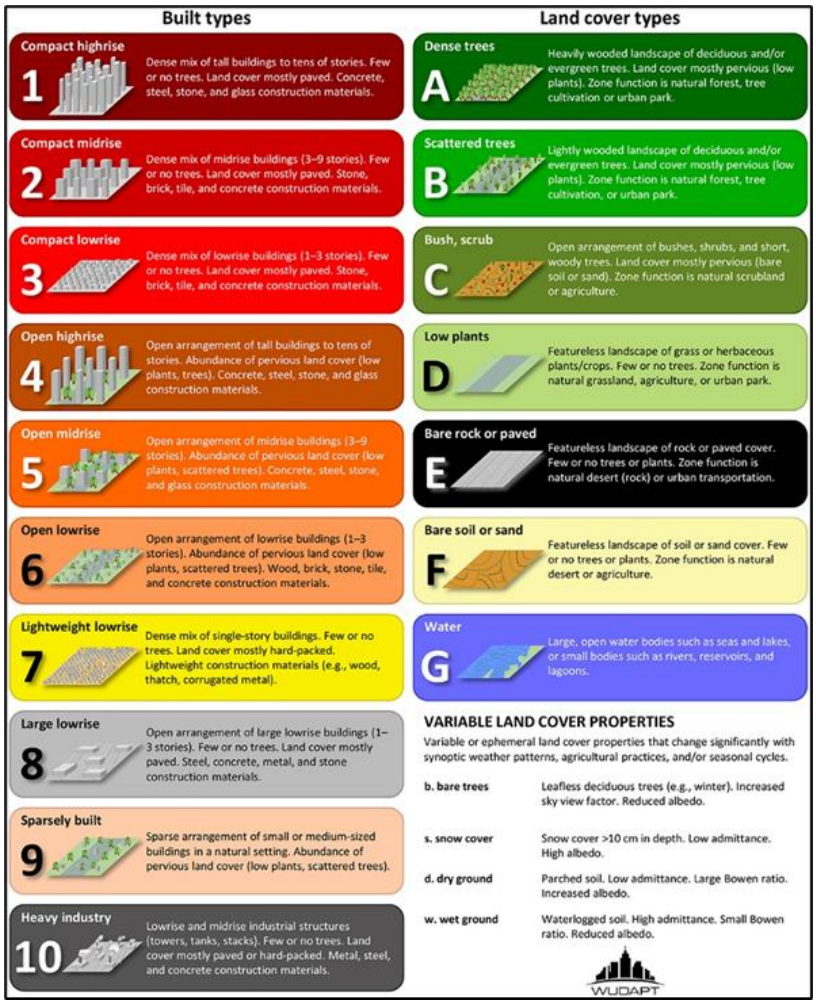

Figure 6: Urban (1–10) and natural (A–G) Local Climate Zone definitions (Stewart and Oke, 2012; Demuzere et al., 2020).

Dublin quite often experiences significant changes in the atmospheric pressure in a very short time, often hour to hour. Pressure changes of 10hPa (10mbar) in less than three hours are associated with the passage over or close-by of strong mid-latitude cyclones, but a drastic 20hPa (20mbar) change in the atmospheric pressure in the same timeframe is not without precedent either. Usually May is the sunniest month, while December is the dullest, but the amount of sunshine varies somewhat even in such a small geographical area as the city. Despite the proximity, the Casement Aerodrome, due to more intense convective cloud formations receives slightly less sunshine than Dublin Airport.

Stewart and Oke (2012) introduced the concept of local climate zones (LCZ) which are defined as the regions that possess similar characteristics like surface cover, structure, material, and human activity, extending horizontally from several hundred meters to kilometres. LCZs (Figure 6) can be divided into 17 standard classes 10 for built-up (compact high rise, compact low rise, open low rise, heavy industry) and 7 for vegetation (dense trees, scattered trees, bare soil, water) with different microclimatic conditions.

Figure 7 illustrates the Local Climate Zones of Dublin, highlighting the predominance of suburban areas (LCZ 6) alongside the compact city centre (LCZ 2). For a clearer interpretation of the spatial structure of the urban heat island (UHI), Dublin city can be conceptualized in concentric layers: the City Centre (LCZ 2) at the core, encircled by the Midtown (LCZ 3–5), followed by the Suburbs and Estates (LCZ 6), and finally the Urban Fringe and Industrial Areas (LCZ 8–10). There are some LCZ 2-5 in smaller pockets of Dun Laoghaire, Dundrum, Swords, Tallaght and Leopardstown, but rest of the urban settlements are mostly suburban in the other three local authorities. While there are relatively fewer industrial areas (LCZ 8 and 10) in the Dublin city, there are many industrial zones within three of the LAs such as at Inchicore, Sandyford, Tallaght etc. Apart from the urban core, the Fingal local authority area is predominantly characterised by sparsely built zones (LCZ 9) and areas of low vegetation (LCZ D). In contrast, while Dún Laoghaire–Rathdown and South Dublin local authority areas also include sparsely built and low-plant zones, they additionally contain pockets of dense tree cover (LCZ A) and scattered trees (LCZ B).

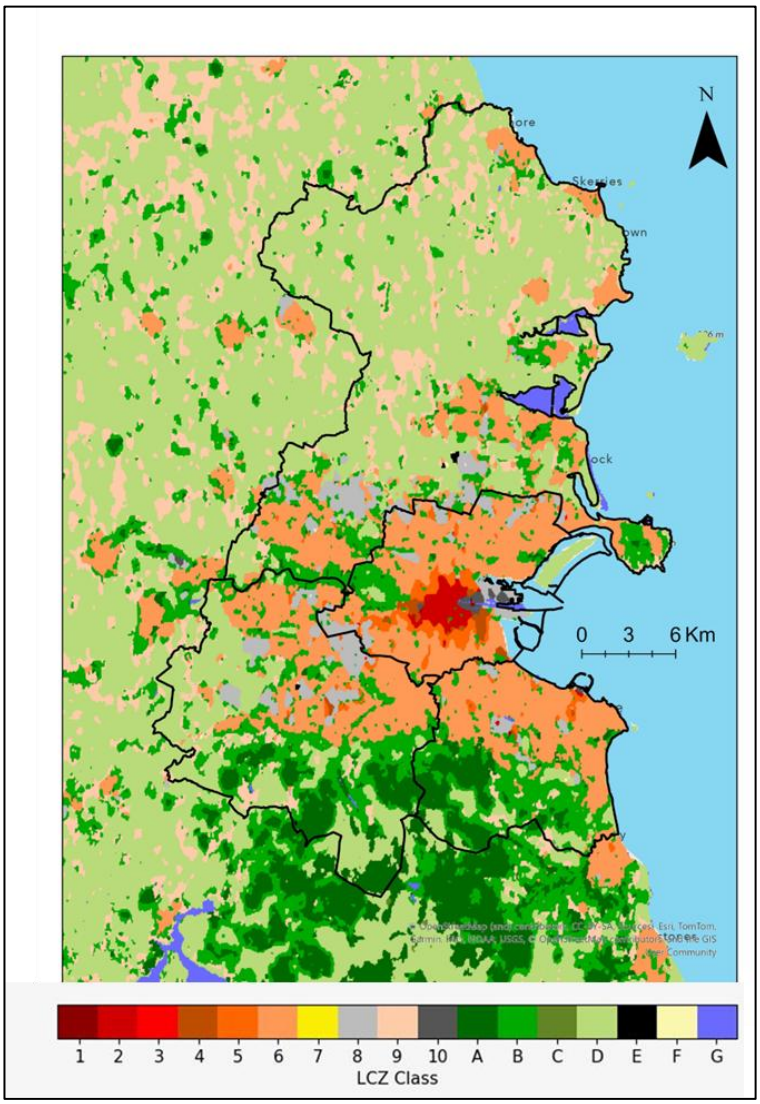

Figure 7: Local Climate Zones of Dublin (Source: LCZ generator map, Demuzere et al., 2021).

2.2 Citizen Weather Station (CWS) network

Citizen weather station units are typically small, battery-powered devices that provide basic information about the atmospheric conditions (air temperature (T), atmospheric pressure (P), relative humidity (RH)); some also record precipitation (P) and wind velocity (V) (figure 7). The modern station is connected to the internet via Wi-Fi, and the owner may choose to share the data acquired on online websites, the best known of which are Weather Underground2 and Netatmo Weather Map3. By collecting data from thousands of stations all around the world, these sites make real-time weather information available at a high spatial and temporal resolution. Official, high-quality stations, such as those on Figure 8 follow WMO guidelines regarding the accuracy of instruments and their exposure; these guidelines stipulate the placement of an instrument shelter at 1-2m above extensive and flat and short grass surfaces. As all such stations follow these guidelines, their observations capture regional scale climate signals. By contrast, private stations using different sensors and do not follow these guidelines; many are in private gardens, attached to walls and roofs. As such, the data that they generate must be evaluated to establish their quality and representativeness. Despite these issues, it is possible to create a citizen weather station (CWS) network that can be used to assess the UHI.



Figure 8: Examples of the temperature sensors from met stations (left) and CWS (right)

In this study, CWS data is obtained from the citizen-database which was first introduced in Kittner et al. (2021). The Crowd-Database development was continued as part of the ENLIGHT project for efficient quality control for any available new data (Fenner et al., 2021). The Crowd-Database mostly contains hourly values of the air-temperature and relative humidity from Netatmo Crowd Weather Station (CWS) from 2019 until the present covering over 500 cities worldwide. Data from the Crowd-Database (citizens) has already been used in a variety of studies e.g. to understand nocturnal heat island advection, surface and canopy layer UHI intensities (Krelaus et al., 2023) and role of urban form in land surface temperature dynamics (Nasreikia et al., 2023)

2.3 Data processing and quality control

The air-temperature data in the Netatmo Crowd-Database has been quality-controlled which assigns quality flags (e.g. location, height, temporal availability and sensor lags) to each hourly measurement (Fenner et al., 2021). Additional geospatial information is added to the data e.g. Global map of LCZs (Demuzere et al., 2022). In the present study we will be analysing temperature data available from the Netatmo CWS where all sensors are identical and accuracy (± 0.3 K) and sensor characteristics, e.g. time lags introduced by the sensor design have been studied extensively (Büchau, 2018; Coney et al., 2022; Mandement & Caumont, 2020).

[2] https://www.wunderground.com/
[3] https://weathermap.netatmo.com/

For Dublin county, the first step of the data evaluation processes was the identification and removal of stations units with insufficient data availability. The location of the CWS stations is shown in the Figure 9. Table 2 provides the details of the stations available for various years categorized by LCZ types.

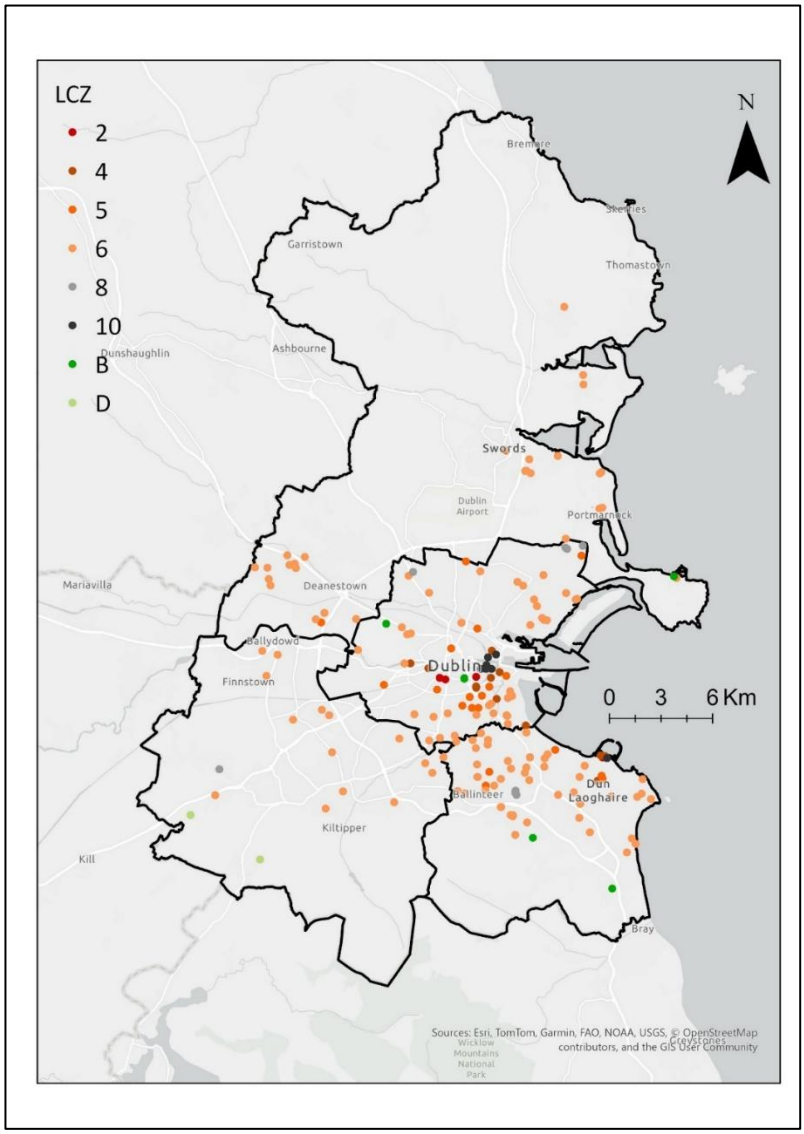

Figure 9: location and LCZ classification of the Netatmos stations used in the present study.

There were 196 CWS stations within the Dublin boundaries. As the data is non continuous/sporadic in 2019 and 2024, in this study we have focussed on the years 2020-2023 and only the stations which had at least 50% data were selected for analysis. Following the application of data quality control/assurance procedures, data from 131 stations comprise the CWS network (Figure 9) and the details about these stations are provided in Appendix A.

The majority (83) are in suburban areas consisting of 2-3 storey terraced or semi-detached houses with large green fractions and a low fraction of impermeable paved surface cover; these areas correspond to a Local Climate Zone (type 6) of open low-rise according to Stewart and Oke (2012). Figure 10 shows the example of available data for temperature from two representative stations. (Harold Cross and Rathmines) for Jan 2020-Dec 2023.

Table 2: Stations characterized by LCZ and Data availability. The final number of stations used after data quality check per year is also mentioned.

	Data Availability				
131	**LCZ**	**Represents**	**Number**	**Year**	**Number**
	LCZ2	**City centre**	7	2019	61
	LCZ4	**Midtown**	8	2020	74
	LCZ5	**Midtown**	9	2021	77
	LCZ6	**Suburbs**	83	2022	76
	LCZ8	**Warehouses/industries**	6	2023	79
	LCZ10	**Industrial area**	8	2024	38
	LCZ B	**Scattered trees**	8		
	LCZ D	**Low croplands**	2		

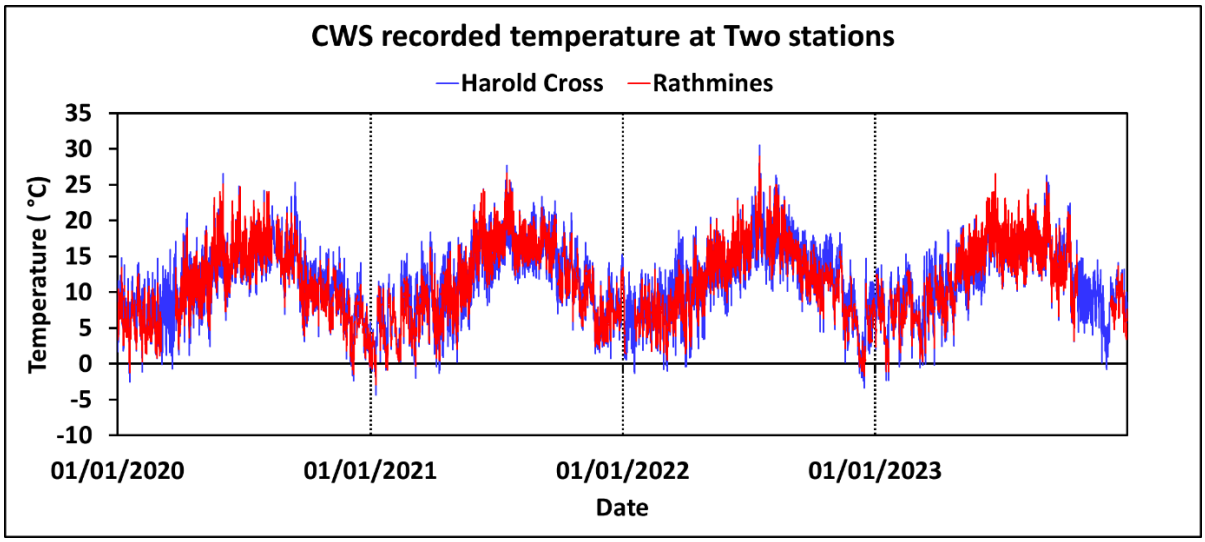

Figure 10: Available temperature records at two stations during 2020-2023

Compared to other, similar networks, the designated CWS net of Dublin was quite small with a low station-count. The comparable study of Chapman et al. (2017) utilised dozens of Netatmo stations in the study of the UHI of London, whereas the research of Meier et al. (2017) used data from well over a hundred AWS. The low number of stations of Dublin was partially due to the relatively small number of continuous AWS, the smaller study area and partially the loss of a considerable percentage of stations during the quality assurance, quality control procedures.

3. UHI Climatology

We generated the hourly averaged, monthly temperatures over the period 2020-2024 for all stations in the CWS network and the three Met Éireann stations. The climatology at Harolds cross, and Phoenix Park are shown in figures 11 and 12. The yearly images reflect the sunlight hours bounded by the average sunrise and sunset times for Dublin. Due to the latitudinal location there is huge variation in the averaged sunlight hours where they could be as high as 16.33 hours in July while only 8 hours in December.

For the three representative stations (Table 3), higher temperatures occur in the summer months when the days are much longer while winters are colder with shorter sunlight hours. The mean maximum temperatures occur 2 h after noon while the minimum temperature in any month is generally around dawn. In all the four years, the maximum temperature is in July while the minimum temperature occurs in the month of January.

Table 3: Maximum and minimum hourly averaged temperature for 2020-2023

Maximum Temperature (°C)				
	2020	**2021**	**2022**	**2023**
Harold Cross	18.3	20.8	21.3	19.5
Rathmines	18.9	20.8	21.3	20.6
Phoenix Park	17.4	19.5	20.3	18.5
Minimum Temperature (°C)				
	2020	**2021**	**2022**	**2023**
Harold Cross	4.7	3.7	4.6	5.7
Rathmines	4.0	3.7	3.7	5.3
Phoenix Park	4.0	2.4	3.9	6.1

The mean diurnal temperature range is higher in the summer months (6.8 °C in July) than in winters (2.7 °C in January). The summer nighttime temperatures are higher than the winter daytime temperatures. For example, in 2022, the averaged minimum temperature in July is 16.6 °C while the averaged maximum temperature in December is about 7 °C. There is a slight warming trend that appear within the first three years but isn't very prominent in 2023. Similar patterns and trends are observed at all the CWS stations and the three met stations.

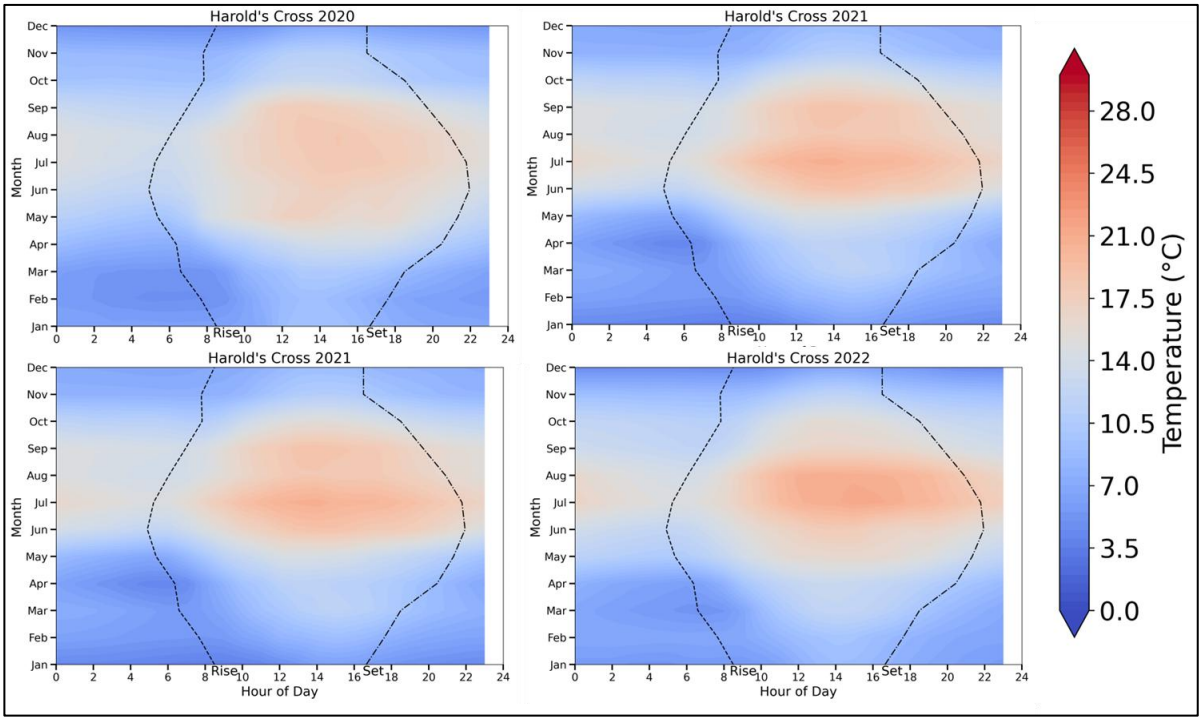

Figure 11: Hourly averaged monthly temperature for CWS suburb station (Harold's Cross) for 2020-2023

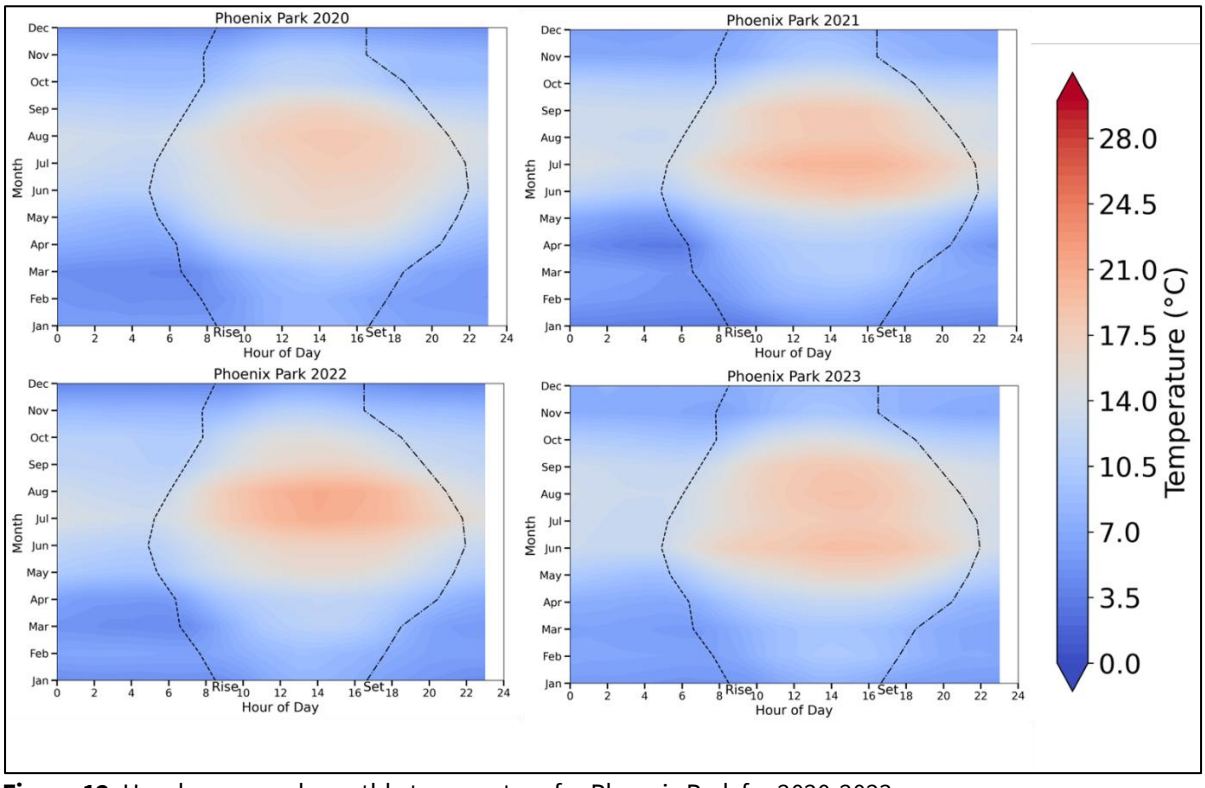

Figure 12: Hourly averaged monthly temperature for Phoenix Park for 2020-2023

Further the climatology of the mean UHI intensities is analysed where the UHI is calculated as the difference of the mean temperature values at any station and corresponding values at a reference met station (Phoenix Park). The hourly averaged UHI intensity of some representative suburban station (Harold Cross, Rathmines, Merrion Park, Ward Hill and Coolock) are shown the figures 13-17. For all these 5 stations, the mean UHI intensities are higher in the nighttime particularly in the summer months while negligible in the winter nights. The nighttime UHI appear few hours after sunset and starts developing

from spring (April) and reaches its maximum value in summer months of July and August. The highest mean UHI intensities are around midnight while the lowest UHI occur just after sunrise for most of the year. The nocturnal UHI is constant owing to much stable atmospheric boundary conditions but begin to disappear after the sunrise when the atmospheric layers start getting mixed. The highest mean UHI is observed are in the range of 3.5-4.3 °C for the midnights of July and August month. The daytime UHI though not as pronounced at the nighttime values also develop in the afternoon hours throughout the year confirming the impact of urban fabric on the increased temperatures in the suburbs. There nocturnal mean UHI at this suburb remains around 3.5°C for all the four years and doesn't reflect any strengthening or weaking trend.

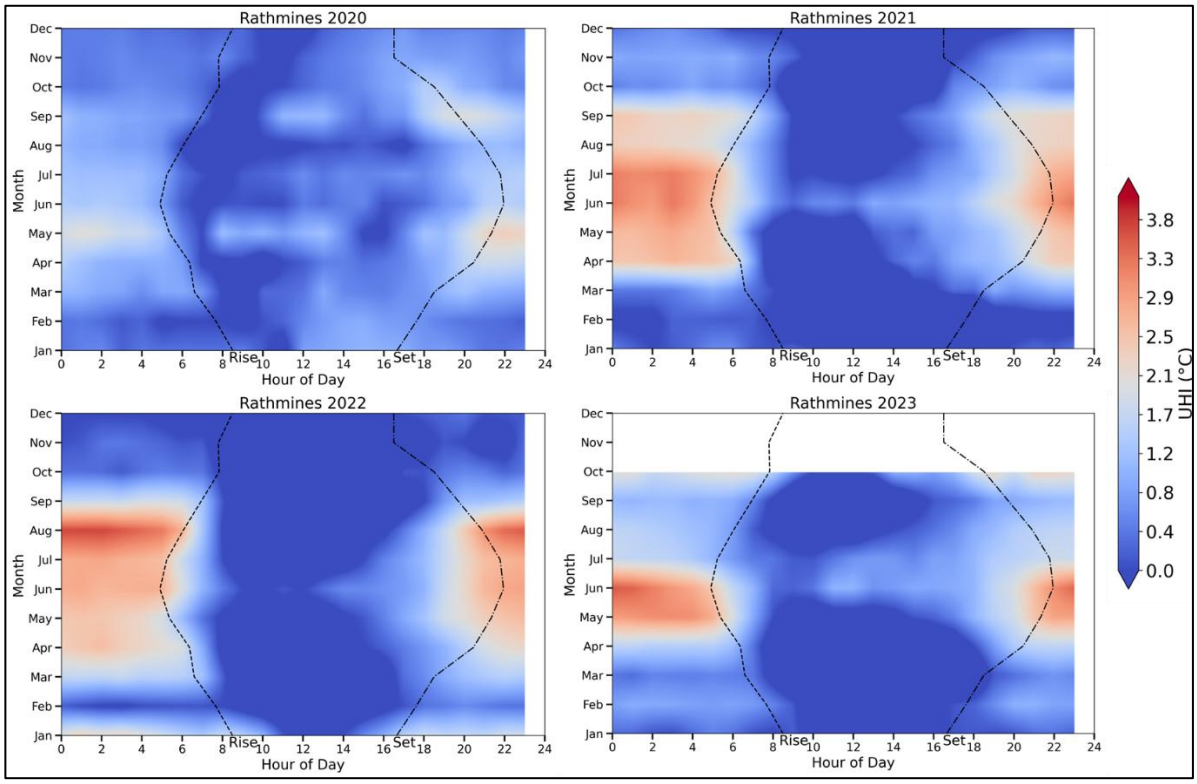

Figure 13: Hourly averaged Monthly UHI for the suburb station (Rathmines) for 2020-2023)

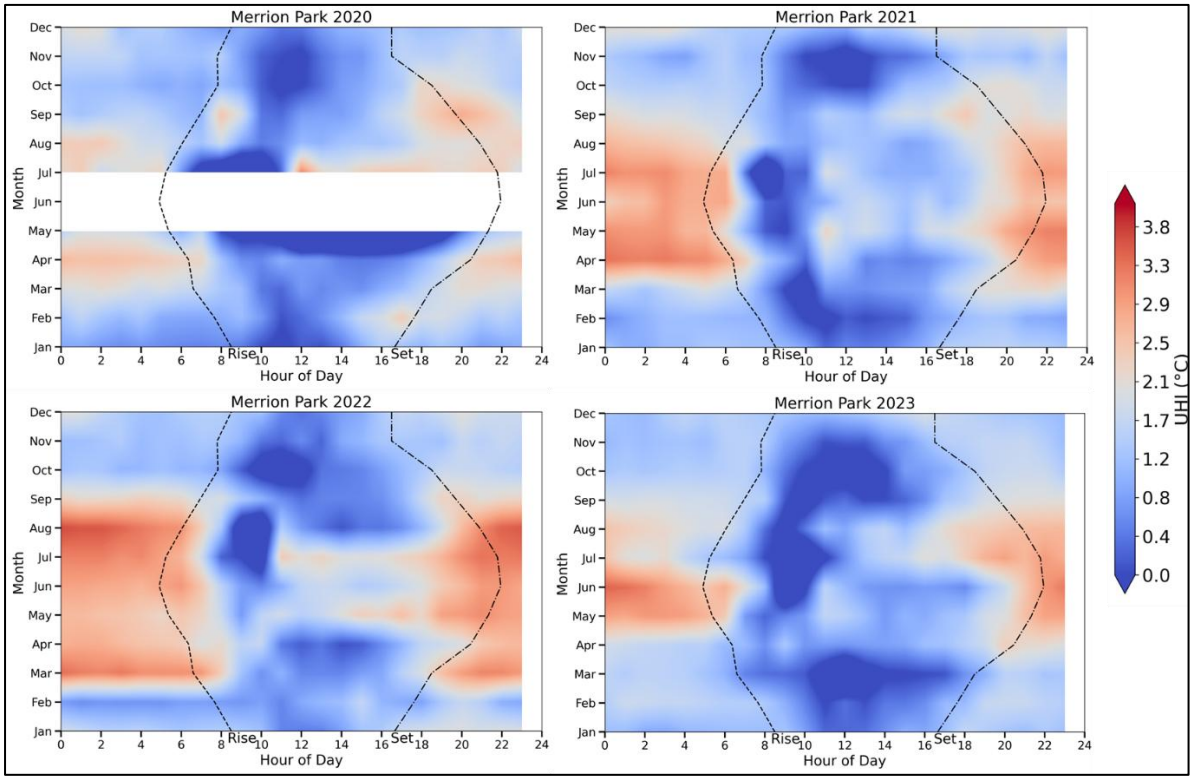

Figure 14: Hourly averaged Monthly UHI for the suburb station (Merrion Park) for 2020-2023)

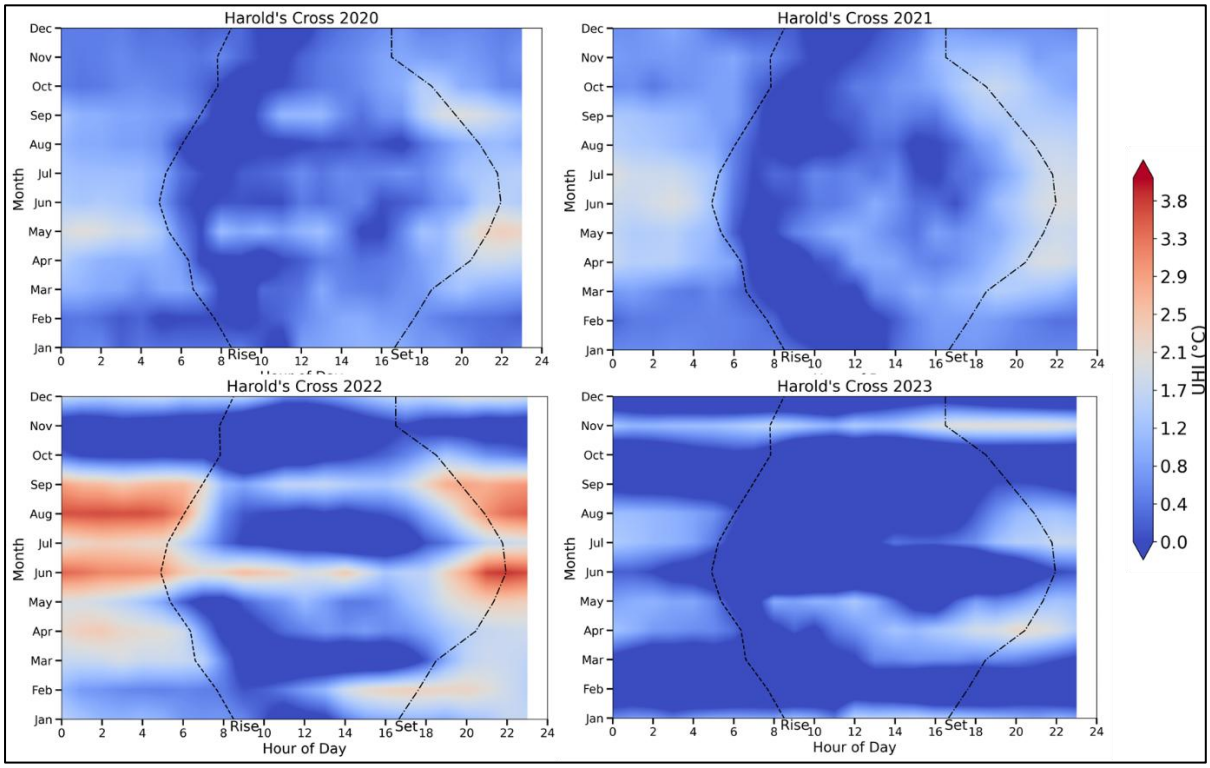

Figure 15: Hourly averaged Monthly UHI for the suburb station (Harolds cross) for 2020-2023)

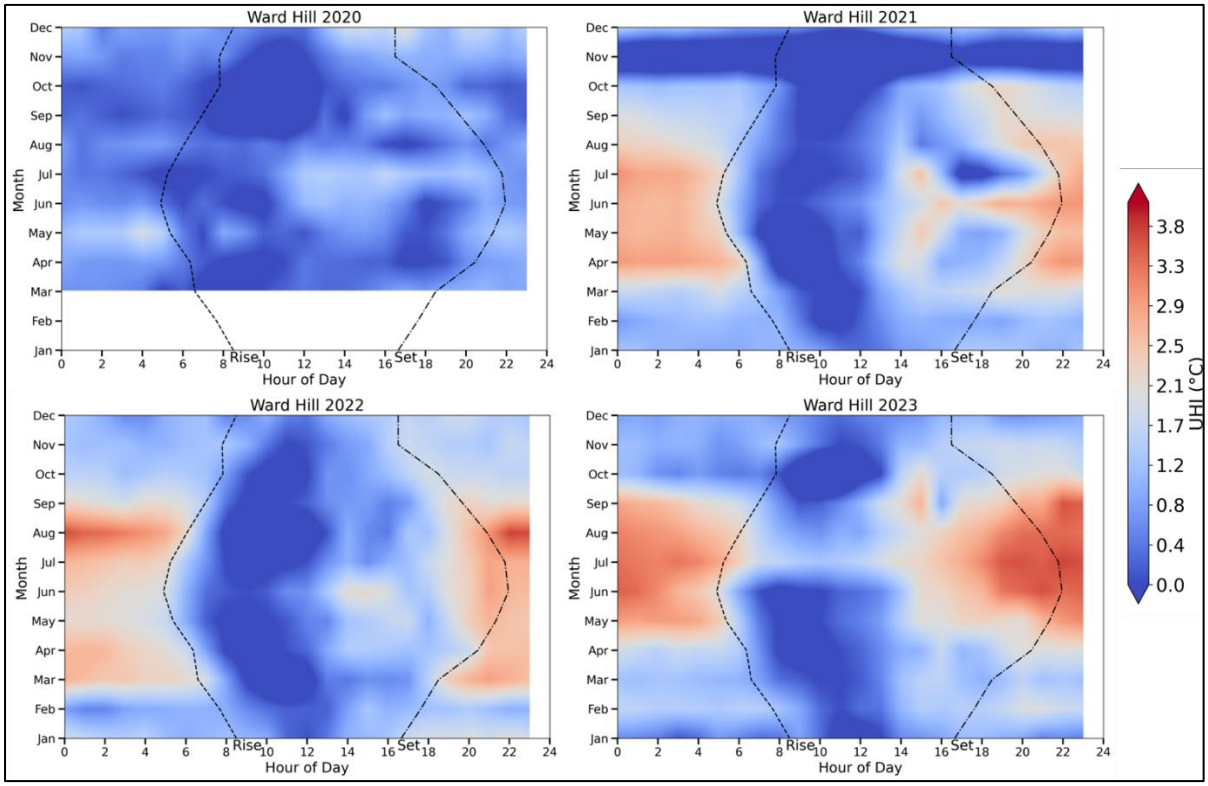

Figure 16: Hourly averaged Monthly UHI for the suburb station (Ward Hill) for 2020-2023)

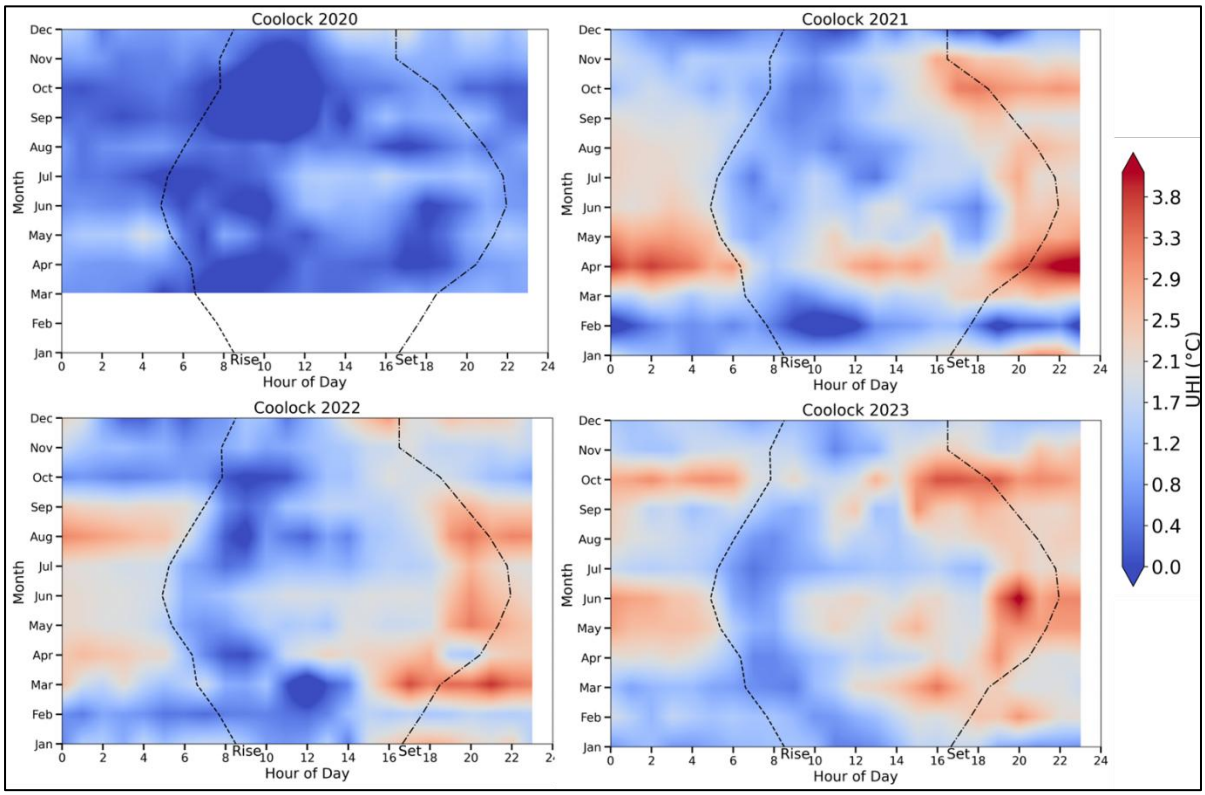

Figure 17: Hourly averaged Monthly UHI for the suburb station (Coolock) for 2020-2023)

4 Summertime UHI

4.1 Selection of Days

As the nighttime UHI is maximum in the summertime, we focus on the three months June, July, August (JJA) for 2020-2023. We have also examined the Lamb weather types (LWT) during the summer months. The LWT scheme is a well-known synoptic classification of daily weather patterns developed by Hubert Lamb, a climatologist. LWT scheme recognizes 27 types of flow and 7 main types of circulations viz., anticyclonic (A), cyclonic (C), northerly (N), easterly (E), southerly (S), westerly (W), north westerly (NW) and the unclassified type (U). LWT has been used extensively to analyse the seasonal and annual variations of climate across the British Isles (BI) (Jones et al., 2013). Fealy and Mills (2018) generated a LWT classification centred on Ireland (LWTIR), providing a register which is a more appropriate synoptic classification for studying weather and climate conditions in Ireland. We focus on anticyclonic conditions (LWT A) which is associated with calm conditions and is favourable to evaluate the impact of urbanized landscape separated from the heat advection in other conditions. Table 4 gives the frequency of the seven prominent LWT at Dublin airport for the four years where the dominance of LWT A is clearly visible in three years (2022-2022). In 2023 LWT A is complimented by conditions like AW, AN and ANW which are anticyclonic conditions with slight westerly, northerly or north-westerly winds.

Table 4: The frequency of the seven basic LWT categories for summer months

LWT	2020	2021	2022	2023
A	53	96	118	42
C	62	38	30	51
N	28	20	11	12
E	3	2	9	16
S	13	12	6	14
W	46	11	43	48
NW	22	25	15	43

LWT is provided four times per day: 00 h, 06 h, 12 h, and 18 h.

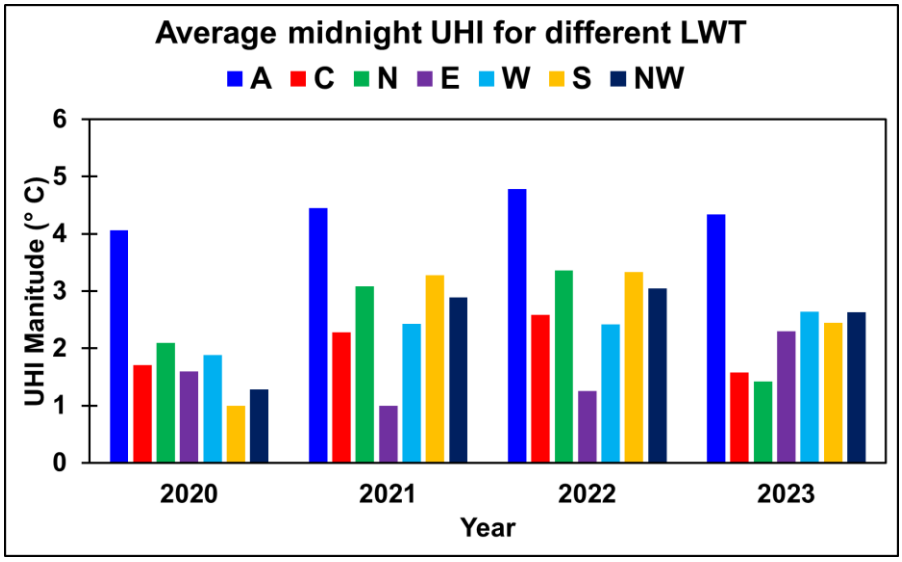

Figure 18: The average summertime midnight UHI associated with different Lamb weather types.

We examined the average summertime midnight UHI for the prominent LWT weather conditions for 2020-2023 in figure 18. This confirms that UHI intensity is greater on anticyclonic (A-type) days, when

calm atmospheric conditions help sustain the phenomenon. We have chosen 10 LWT days for each year for further detailed examination. Table 5 details the 10 days which fall under A category analysed for their UHI intensities for 2021-2023. Here onwards whenever we mention the LWT A days or fair-weather days in the text, we refer to these 10 days of individual years.

Table 5: Fair weather/ LWT A type dates for each year

Year	Days	Dates with LWT as Anticyclonic (A) or fair weather days
2020	10	(8 June), (10,11,19,20,21 July) (3,8,9,20 August)
2021	10	(12June), (15,16,17,18 July), (24,25,26,27,28 August)
2022	10	(13, 22 June) (13,14,15,16, July), (8,9,10,11 August)
2023	10	(21, 22June), (20,21, 26 July), (6,7,8,9 ,16August)

4.2 Diurnal summertime UHI across Dublin

Figure 19 shows the diurnal averaged temperature of the LWT days of summer 2020-2023 categorized for the LCZ types (the City Centre (LCZ 2), Midtown (LCZ 4&5), Suburbs (LCZ 6) and Industrial Areas (LCZ 8 &10)) and compared with Phoenix Park. The values for all the stations within same LCZ are averaged for comparison.

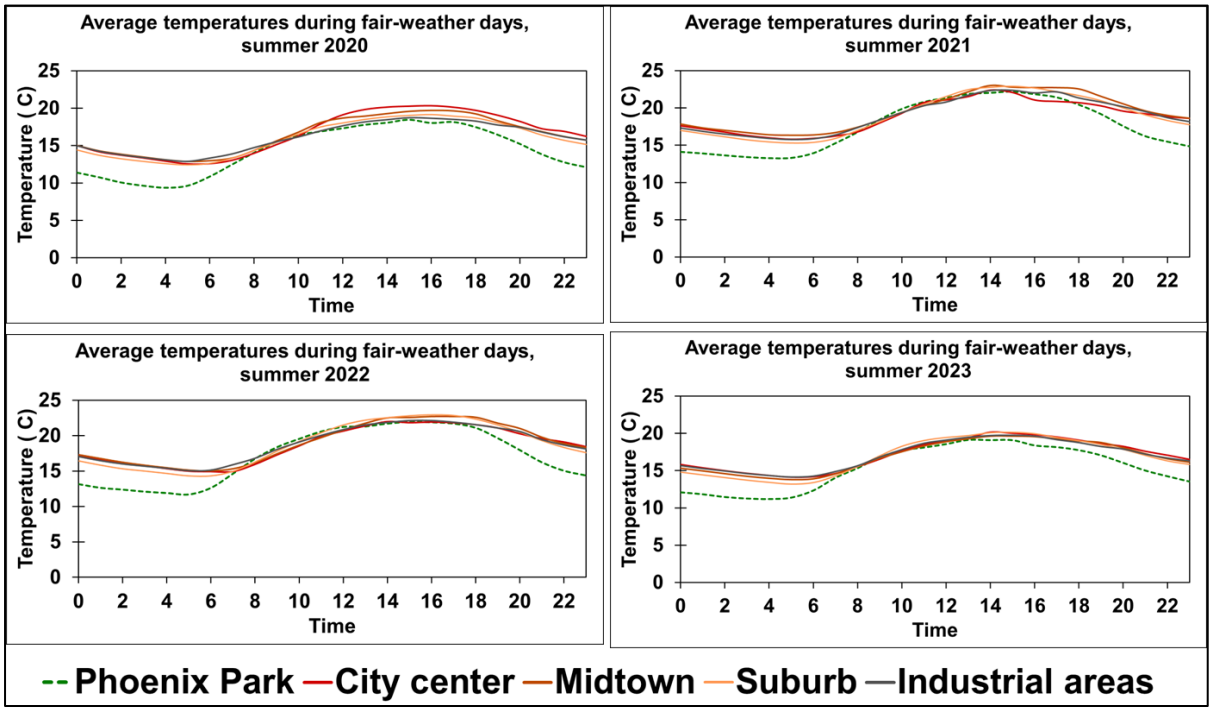

Figure 19: Hourly averaged temperatures for fair-weather days for representative LCZ type and Phoenix Park met station

The diurnal means UHI for the summer season of each year categorized by LCZ type is compared with reference to the temperatures at Phoenix Park in Figure 20. The high UHI differences sustain through the night and start decreasing in the early hours of and dissipate around sunrise. For different LCZs, the nocturnal UHI are around 4 °C in different years where city center (LCZ 2) and midtown (LCZ4&5) show higher intensities than suburbs (LCZ 6). The magnitude of the UHI slightly fluctuated during the daytime (less than 1 degree generally) but becomes more homogeneous in the night hours. These variations in the daytime can be attributed to the location of the CWS monitors e.g. shade effect from the urban/tree

canopy, proximity to irrigated lawns or waterbodies which should be investigated further. Interestingly, there negative UHI occurrences during morning hours for different LCZs is also captured in the CWS data.

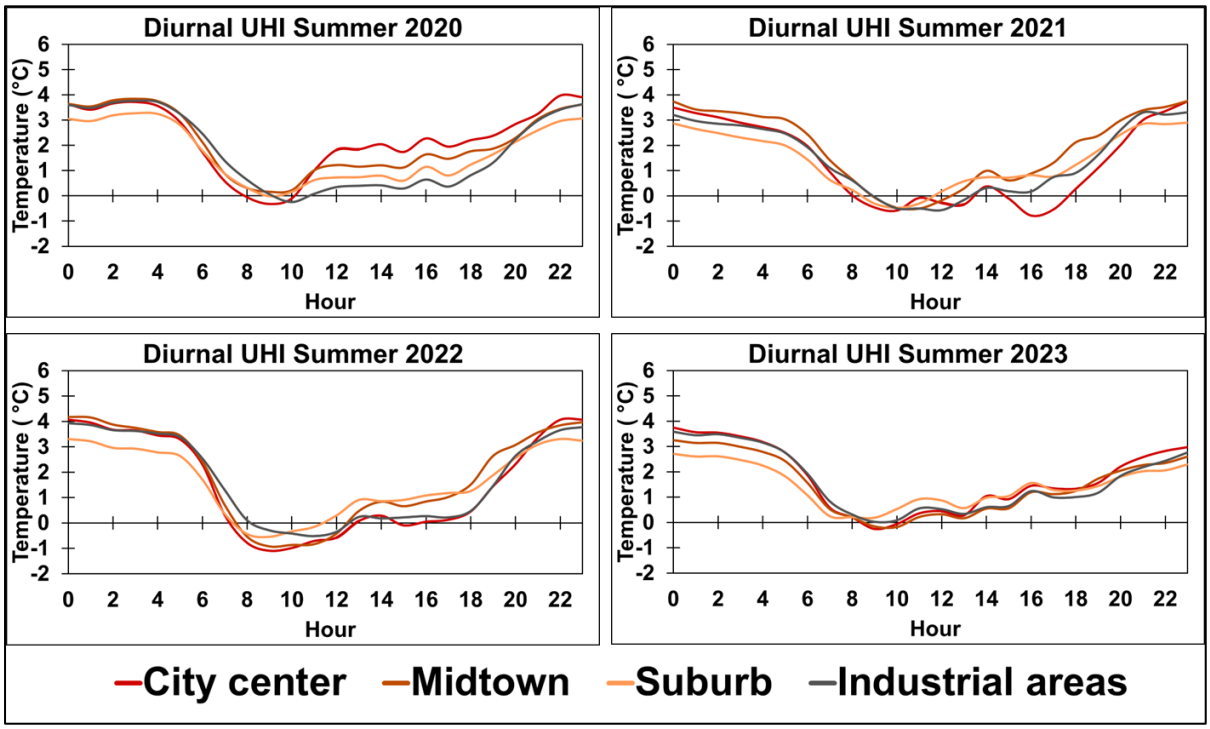

Figure 20: Hourly averaged summer UHI for fair-weather days for representative LCZ type with referenced to Phoenix Park

Figure 21 gives the maximum UHI intensity categorized for the LCZ types for LWT days. It clearly demonstrates that the urban fabric is warmer than the Phoenix park. Again, the highest UHI intensities in different years are observed in city centre (LCZ 2) and midtown (LCZ 4 & 5) and minimum in the suburbs (LCZ 6). These LCZs represent the dense and open arrangement of tall buildings respectively. The land cover is mostly paved, and the steel, stone and glass dominate the building materials. This compact nature of buildings tends to cool slower and retain higher values of UHIs. Industrial areas (LCZ 8 & 10) on the other hand represents low and midrise industrial structures with sparse vegetation. The land cover is mostly paved with metal, steel and concrete as construction material. These buildings also retain a lot of heat and even generate heat during night owing to the industrial processes and hence show higher UHI intensities.

LCZ 6 represents open arrangement of low-rise buildings with abundant green cover. The construction of a typical sub urban home could be wood, brick stone tile and concrete. These areas tend to cool faster than compact concrete buildings both due to the construction material type and smaller size of the buildings. It is interesting to note that within the LCZs the difference in highest nocturnal UHI could be of about 1˚C especially between LCZ2 &4 and LCZ 6. The highest mean UHI intensity of the studied period remain well below the 6.5˚C recorded by Sweeney (1987) and barely exceed half of the 8˚C maximum urban-rural temperature contrast suggested by Graham (1993) for optimal conditions of clear skies and wind speed below 3m/s-1.

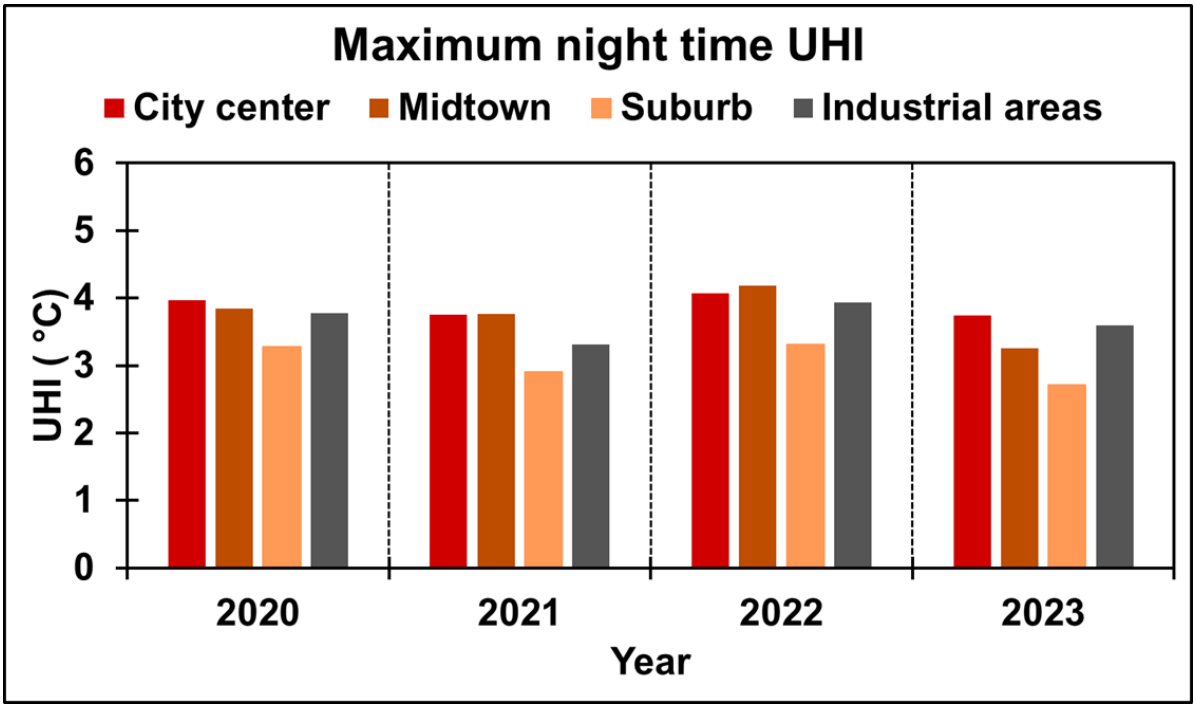

Figure 21: Maximum UHI during fair weather days for representative LCZ at city centre, midtown, suburbs and industrial areas

The genesis and daily life cycle of the UHI is mostly consistent with the examples described in the wider literature (e.g.: Oke, 1982 or Oke, Mills, Christen and Voogt, 2017) where the maximum UHI intensities were recorded two-three hours after sunset for the four years. The differences in the temperatures between the residential areas (urban) and the measurement sites by the hourly averaged cooling rate. All CWS station (LCZ 2-10) are considered as urban, and Pheonix park provides the rural/reference conditions.

The cooling rate (Figure 22) is calculated as the difference in the temperature values at the hour and its preceding hour and is normalized for sunset time. For fair weather days, the figure shows that for all the years the urban stations cool slower than the reference station from late evening to midnight. The cooling of Phoenix Park is faster than the urban areas where it is much linear. This agrees well with the findings from Oke (1982) that the cities with complex urban fabric cool down slowly than the rural areas with open expanse and more vegetation. The compact structure of the urban fabric results in slower energy dissipation to the background as compared to vast open expanses. Phoenix Park warms more quickly than the urban stations in the morning, resulting in an urban cool island effect typical of early hours in a city. This can also be attributed to having lower albedo than the urban fabric which facilitates increase warming in the open settings

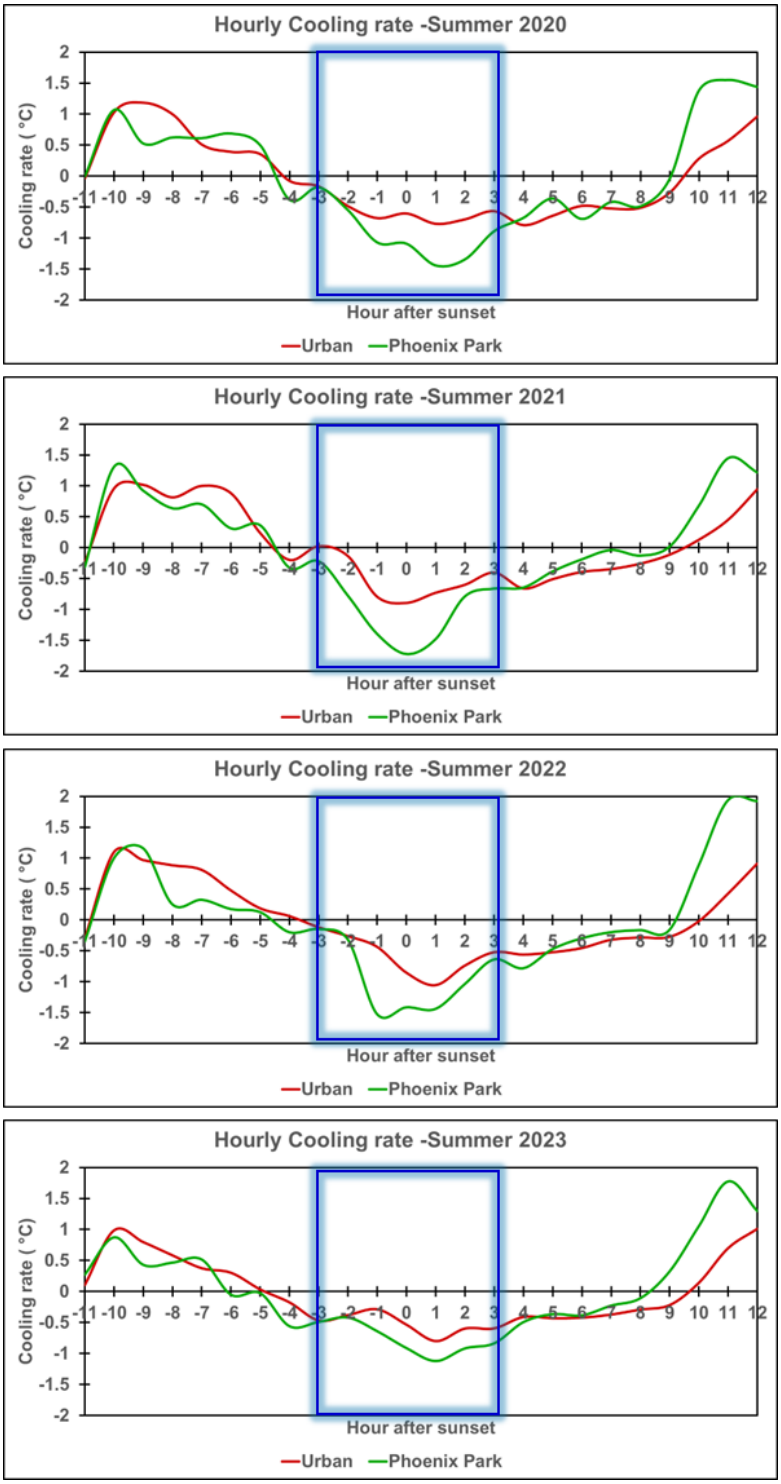

Figure 22: Averaged hourly cooling rates of the Phoenix park and urban stations around Dublin

4.3 Nocturnal UHI maps

The UHI maps generated for fair weather days at midnight are shown in Figure 23. These maps reveal that the entire urban fabric of Dublin is much warmer than Phoenix Park. The UHI intensities are generally low over much of the less densely built and relatively homogenous urban areas (extensive suburbs with detached, semi-detached and terraced houses) towards the more densely built centre where the temperature readings begin to rise steadily again towards the UHI 'peak'. The primary UHI 'peak', regardless of the UHI intensity approximately coincide with the historical city centre and the

south-central area. The city centre is almost 3 to 5 degrees warmer in all the four years when compared to Phoenix Park. Similar hotspots are visible in dense urban and suburban areas of Dun Laoghaire, Dundrum, Coolmine, some prominent industrial zones viz., around Ballymun, Clondalkin and Tallaght.

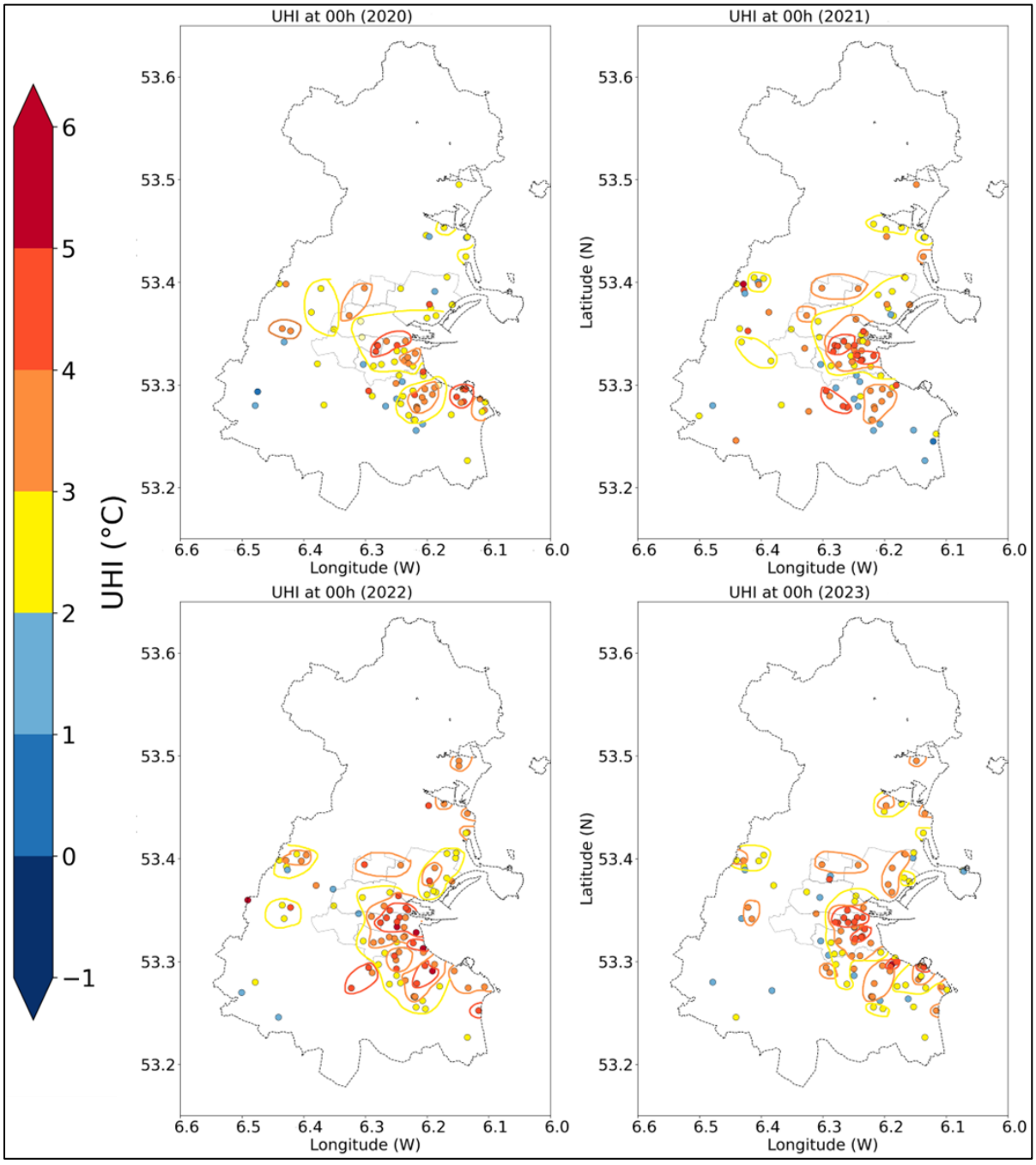

Figure 23: UHI spatial plot averaged at 00h of the 10 LWT A days for each year

Unlike some of the earlier works which utilised mobile measurements (Sweeney, 1987 or Graham, 1993), the temperature records of the present study did not detect any other cold pools or cold air flows in the major river valleys embedded in the urban fabric. This issue is likely the result of the spatial resolution of the CWS network and the location of the individual units. This urban-rural temperature contrast mirrors the conclusions of the study of Dublin's UHI from 2014 carried out by Alexander and Mills (2014).

4.4 Modelled UHI for Dublin

Currently, Numerical Weather Prediction (NWP) models are widely used by the scientific community to attain a reliable forecast of meteorology (Brotzge et al., 2023; Jimenez et al., 2018; Powers et al., 2017). NWP such as the Weather Research and Forecasting (WRF) model is a widely used mesoscale model which has been extensively used in the fields of weather and climate, urban heat island, extreme weather events, regional climate simulations across the globe (Nolan et al., 2017; Sati and Mohan 2018; Vogal and Ashfari 2020; Zhu and Oko 2023). Appendix B presents the high-resolution WRF modelling framework used to simulate Dublin's UHI in May 2020. The setup is described comprehensively, covering synoptic conditions, domain configuration, integration of CORINE land cover and LCZ data, and ERA5 reanalysis inputs. Validation against observations demonstrates strong agreement, with statistical tests confirming the model's reliability.

WRF simulated UHI is assessed for the three days 14-16 May 2020 which corresponded to dominant LWT A synoptic conditions reported for Dublin (Fealy and Mills 2018). The wind speeds were generally low for most of the three days (<3m/s) which correspond well to anticyclonic (fair-weather) days. The UHI was calculated across the study region with Phoenix Park as the reference station. The diurnal variation of the model simulated UHI averaged for the station representative of LCZ is shown in Figure 24. These diurnal variations depict the genesis of the UHI typical to any urban area as mentioned in Oke et al., (2017). Due to a well-mixed atmosphere during daytime, the temperatures are similar across the city with a marginal difference. The UHI phenomenon is stronger few hours after sunset and sustains at nighttime. This reasons for the subsistence of this nocturnal UHI phenomenon is both due to slower cooling rates of the urban fabric and a much stable nocturnal boundary layer. This genesis is discussed in detail in the next section.

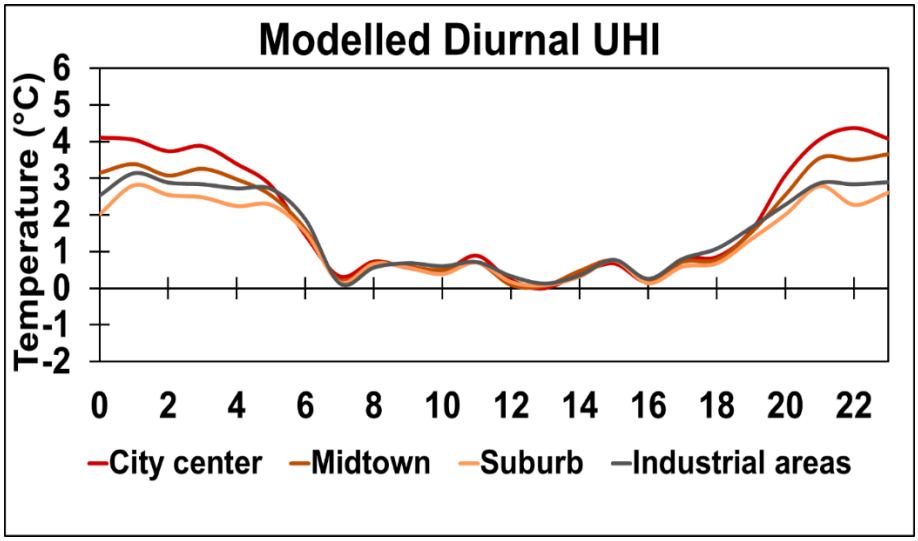

Figure 24: Modelled Hourly averaged UHI for the three days for different urban areas.

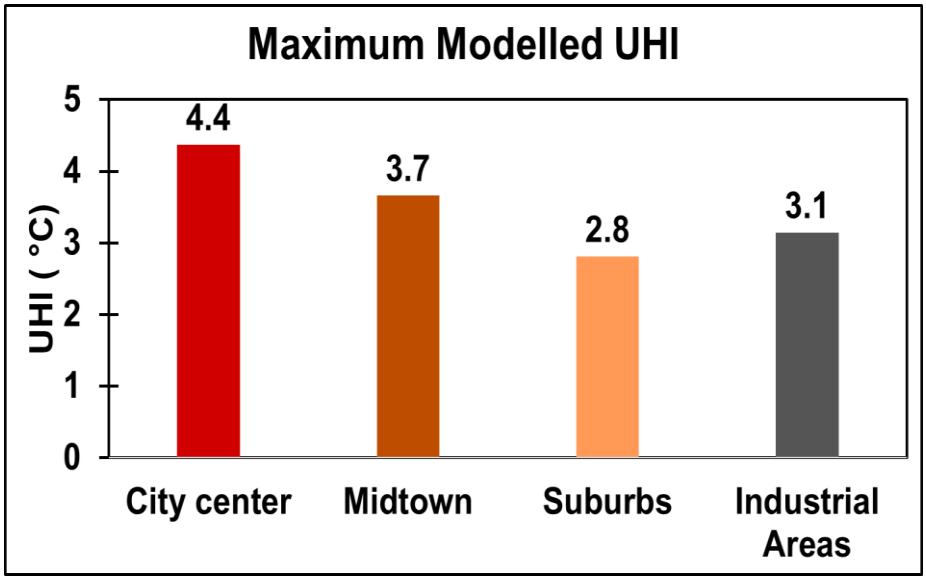

Figure 25: Modelled maximum nighttime UHI for different urban areas referenced to Phoenix Park.

The modelled maximum UHI intensity for each LCZ is depicted in Figure 25 which reflects the findings from the CWS earlier. The city center (LCZ 2) and midtown (LCZ 4 & 6) have higher nocturnal UHI intensities when compared to the suburbs (LCZ 6). Similarly, the modelled maximum UHI also show higher values for LCZ 8 & 10 which represent the industrial site.

The formation and genesis of UHI across the study region relative to Pheonix park is shown at selected hours in the Figure 26.

At 12:00: A well-mixed boundary layer leads to a homogenised temperature with little or no UHI (±0.5 °C) across the city. Irish sea which lies to the east of Dublin is cooler than the land during daytime and this effect is visible along the coast where the cool zone appears. This cool zone is due to to the land-ocean temperature differences and not related to the urban fabric. The Dublin Mountains, bordering County Wicklow, remain cooler than the urban areas of Dublin throughout both day and night due to their higher elevation.

At 18:00: This time coincides with the occurrence of maximum daily temperatures. The temperature profile is homogenised across the study region with little or no variation.

At 00:00: The development of UHI is visible at nighttime where the urban fabric is warmer than the surroundings. Figure 26 shows a clear strong heat island of 4.5 degrees in the Dublin city centre. The secondary UHI hotspots (3 °C) can be observed in the denser mixed industrial and suburban locations such as Ballymount industrial estate, Ballycoolan Business Park and Coolock. Both in the north and south of the city across the suburbs the UHI of 2-2.5 °C is observed in areas like Ballsbridge, Portobello, Artane, Rathmines, Cabra etc. Across the other LAs the urban areas such as Dun Laoghaire, Swords, Stillorgan. Dundrum. Tallaght, Balbriggan, Donabate, Rush, Lusk etc are warmer than their surroundings.

The urban parks viz., Phoenix park, St Ann's Park, Tymon Park, Irishtown Nature Reserve appear to be cold pools of negative heat island that resounds with the phenomenon identified in the wider literature as 'cold pools' (see, e.g., Oke, 1982; Taha, 1997; Oke, Mills, Christen and Voogt, 2017). These were 1-2 degrees cooler than the city centre at nighttime. This clearly indicates the importance of green spaces in mitigating the UHI intensities in the cities. Howth due to its higher altitude than most of the city also appears as a prominent cool spot. Ocean is warmer than land at nighttime so certain areas along the coastline shows the higher temperature which is again due to the land-ocean interactions.

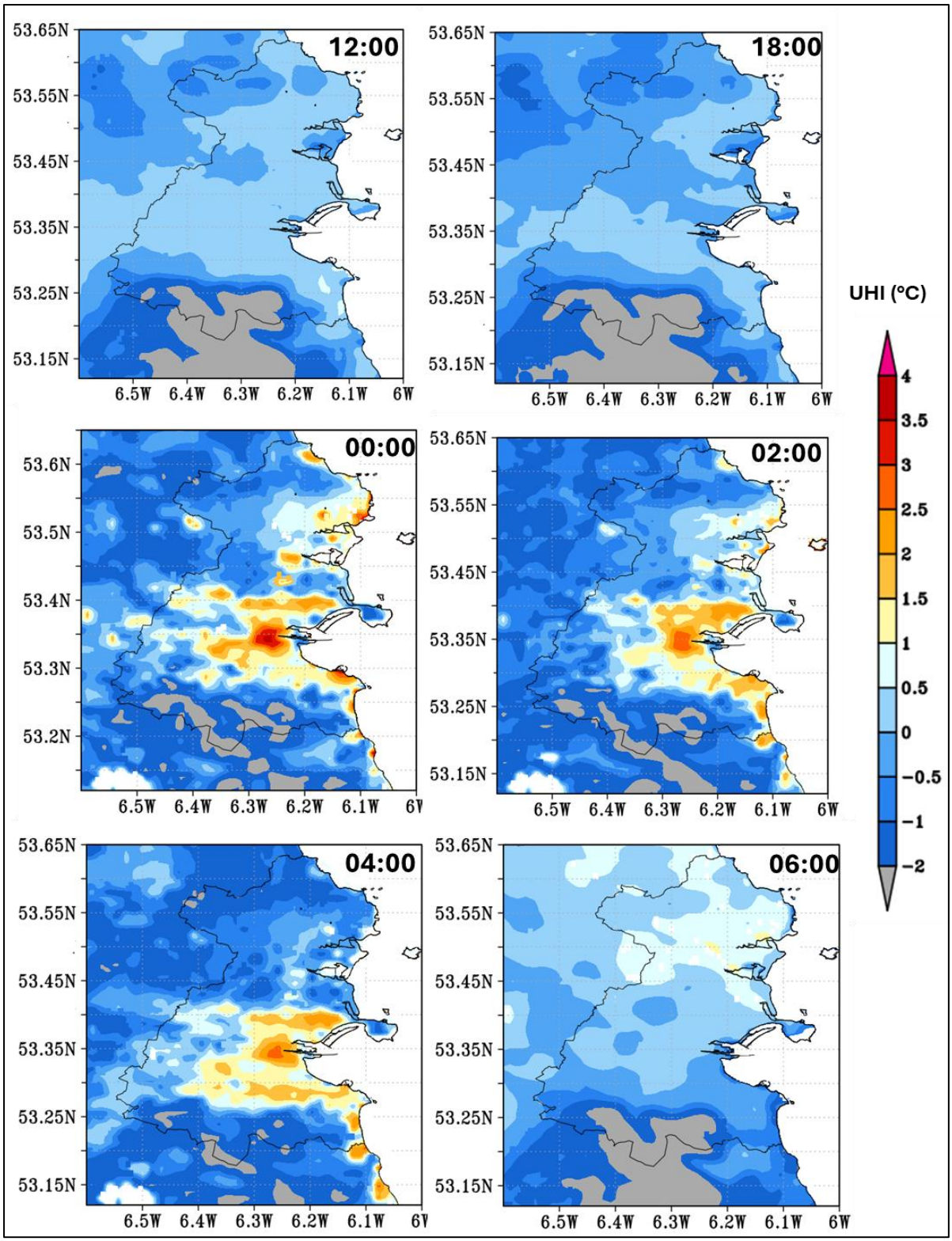

Figure 26: The development of UHI phenomenon across Dublin

02 and 04: Owing to the stable nocturnal boundary layer and the slower cooling rates, the UHI sustains for most part of the night. City centre is still warm with UHI intensities around 3.5 °C and 2.5 °C at 02 and 04 h respectively. Secondary UHI hotspots also sustain but the heat intensity gets lowered. Effect of ocean getting diminished and the coastline also doesn't appear to be warmer and reflects the suburban

UHI intensities. Cold spots become cooler and larger with the night and other small parks, golf courses etc also appear as cool zones.

At 06:00: At the time of sunrise, the stable boundary layer collapse and the UHI collapses across the city. With the availability of sunshine and heat well mixed homogenised boundary layer starts to re develop.

The general features and structure of the urban heat island of Dublin reflects the phenomenon's description in the wider literature (e.g.: Oke, 1982) and closely corresponds with the findings of the three previous major studies on the UHI of Dublin: Sweeney (1987), Graham (1993) and Alexander and Mils (2014).

4.5 Satellite based Surface UHI

As mentioned earlier, LST-based SUHI complements canopy layer UHI by capturing surface-driven thermal patterns, while canopy UHI reflects air temperature experienced by people. Together, they link surface heat processes to actual urban thermal conditions.

Using the ECOSTRESS Land Surface Temperature and Emissivity (LSTE) product (ECO_L2T_LSTE.002), the spatial pattern of land surface temperature (LST) across Dublin was analysed at high spatial resolution (~70 m) for the second week of May 2020 (Figure 27). The LST observations used in this analysis correspond to an overpass time of approximately 16:00 (local time), capturing surface temperatures during the late afternoon when solar heating is still active but surfaces have already accumulated heat throughout the day. The dataset was extracted through the AppEEARS platform (AppEEARS 2026), which processes data by identifying relevant satellite granules, mosaicking them, and clipping them to the study area, while preserving geographic coordinates during reprojection.

The resulting dataset captures fine-scale urban–rural contrasts across the Dublin region, with higher surface temperatures associated with dense built-up and impervious areas in Dublin City, as well as urban centres in Fingal (e.g., Swords), South Dublin (e.g., Tallaght), and Dun Laoghaire. Maximum daytime surface UHI (calculated with Phoenix park as reference) intensities exceed 10°C in the most densely built urban cores, while suburban areas typically exhibit elevated temperatures in the range of 6–7°C. In contrast, cooler conditions are observed in vegetated zones and parks, where temperatures are typically 1–2°C lower. The coolest conditions are evident in the Dublin Mountains, where surface temperatures can be up to ~5°C cooler than Phoenix park, reflecting the combined effects of altitude, vegetation cover, and reduced urban influence.

An advantage of ECOSTRESS LST data is its flexible temporal sampling, with overpass times varying due to the (International Space Station (ISS) orbit rather than fixed local times. This captures a range of thermal conditions, from morning cooling to daytime heating, which is particularly useful in Dublin's variable climate. However, comparisons across dates require caution due to differences in acquisition time and atmospheric conditions. The use of QA layers and cloud masks ensures that only reliable data are included in the analysis (Hook and Hulley, 2022).

No cloud-free night-time ECOSTRESS overpass was available that provided complete spatial coverage of the Dublin region during the second week of May 2020, limiting its use for analysing nocturnal urban heat island (UHI) characteristics. Due to persistent cloud cover and fragmented scenes, it was not possible to derive a consistent night-time LST pattern from ECOSTRESS for this period. As an alternative, a MODIS-based 8-day composite LST product (Wan et al., 2021)

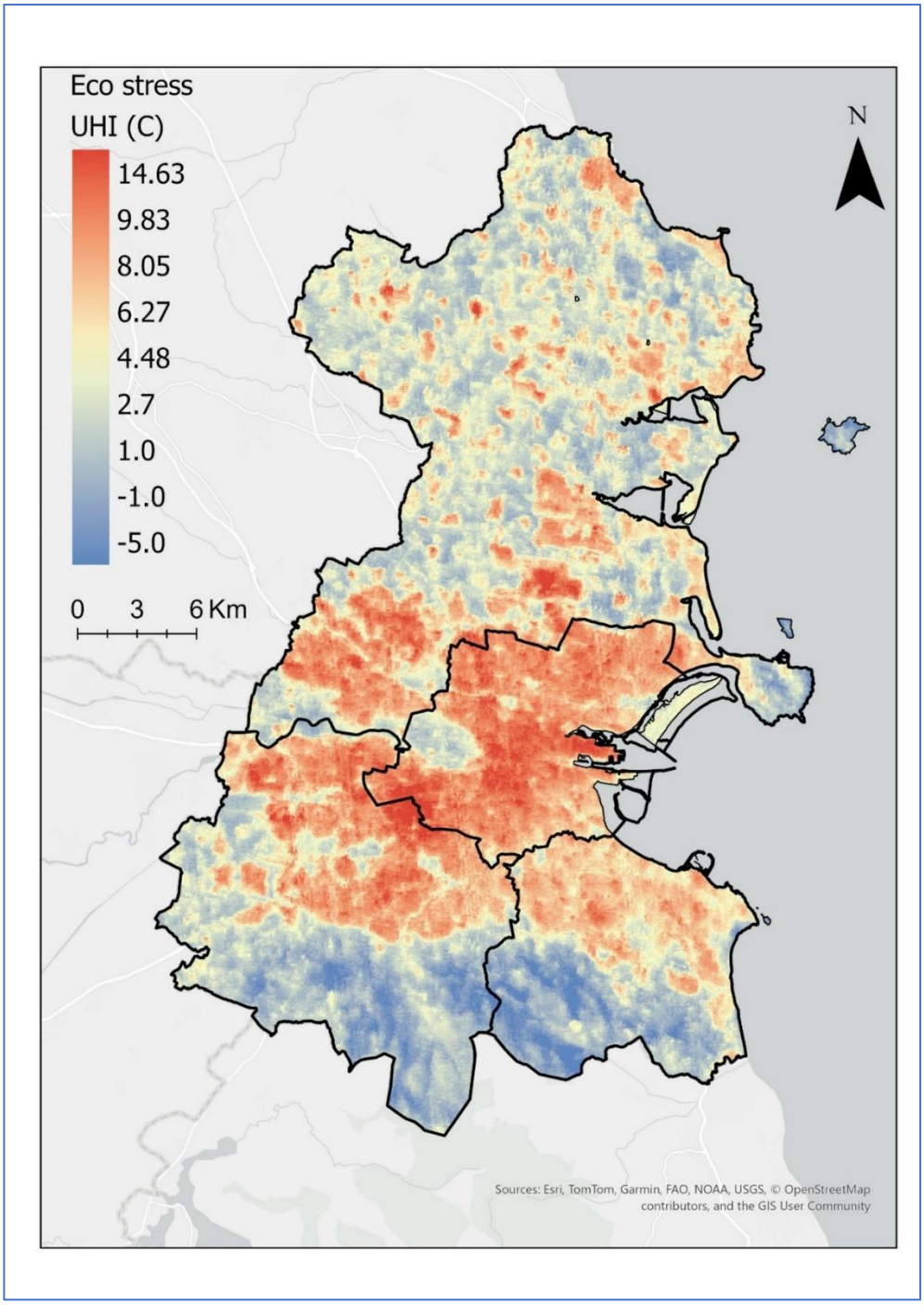

Figure 27: Land Surface Temperature (LST) across Dublin derived from the ECOSTRESS LSTE product at ~70 m resolution for the second week of May 2020 (16:00 local time overpass).

was used, specifically from the Aqua platform with an approximate overpass time of 01:30 (night-time). This timing is particularly suitable for capturing UHI characteristics, as nocturnal conditions minimise the influence of solar radiation and highlight the role of heat storage and release from urban materials. The 8-day compositing approach further reduces cloud contamination and ensures more complete spatial coverage, allowing for a robust representation of night-time UHI patterns across Dublin.

The resulting UHI pattern (Figure 28) shows elevated surface temperatures not only in the dense city centre but also across major suburban centres such as Dún Laoghaire, Swords, and Tallaght. Night-time UHI intensities reach around ~5°C in the city centre and Dún Laoghaire, while suburban areas typically

exhibit lower intensities of ~1–3°C. Industrial zones show elevated values of ~3°C or more, reflecting extensive impervious surfaces. These areas appear warmer due to their urban fabric, characterised by impervious surfaces, commercial zones, and residential density, which enhance heat absorption and storage. It is important to note that this reflects land surface UHI rather than canopy-layer UHI; therefore, the pattern highlights surface heating effects driven by land cover and material properties. As a result, even suburban centres with moderate density can exhibit strong LST signatures, In contrast, urban green spaces such as Phoenix Park are approximately ~1°C cooler, while elevated and less urbanised areas such as the Dublin Mountains are more than ~2.5°C cooler, again highlighting the combined influence of vegetation, elevation, and reduced urban density.

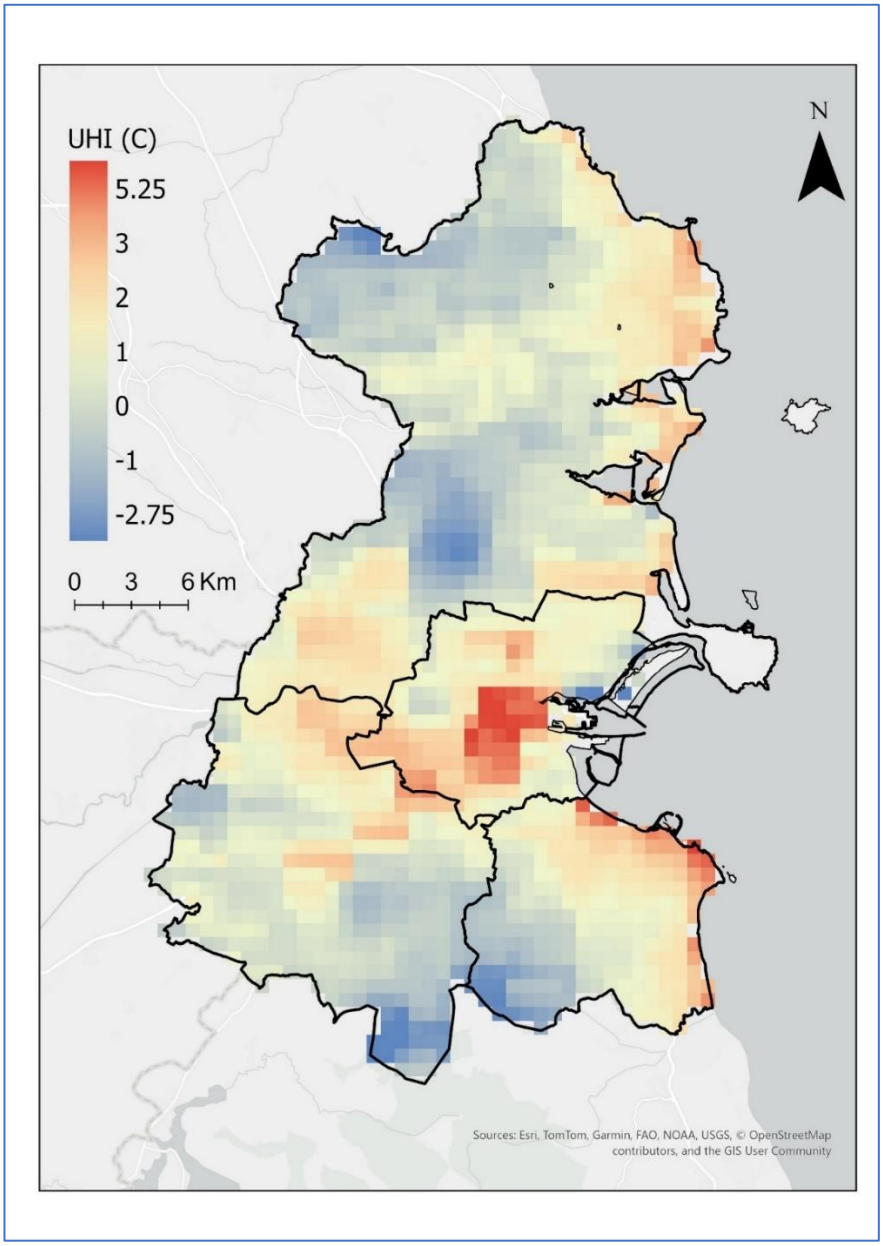

Figure 28: Night-time land surface temperature (LST)-based UHI pattern across Dublin derived from the MODIS Aqua 8-day composite (01:30 local time) for the second week of May 2020.

5 Implications of Urban Heat Island and Policy recommendations

5.1 Degree days

A degree day (in °C) represents the number of degrees by which the average temperature of a day has gone above or below the reference temperature values (UK Met office). Degree days can be distinguished as cooling degree days (CDD) in the summer season and heating degree days (HDD) in the winter that reflect the energy need to cool or heat a building in these seasons respectively. The threshold value for CDD and HDD is 22.0 C and 15.5 C respectively (EPA).

A cooling degree day is said to occur when the outside temperature is warm enough to require cooling inside (i.e. in a building/dwelling). Essentially the difference between the mean temperature of day and the threshold value indicates the cooling degree days. Degree days are also included as one of the Ireland's climate resilience policy indicators and for Dublin CDD is calculated based on the observations from Dublin Airport (DAP). In Figure 29 we compare the CDD for the summer days of 2020-2023 at DAP and the LCZ stations. Interestingly the CDD are zero for all the years at DAP and the LCZs in 2020, but they begin to appear (3+days) in various LCZs for different years. The CDDs are very low or negligible for Dublin and no significant trend is observed within the data of four years. The calculation does raise the concern that this policy indicator should be reported for actual residential areas such as LCZ4 or LCZ 6 within the city rather than the values at airport.

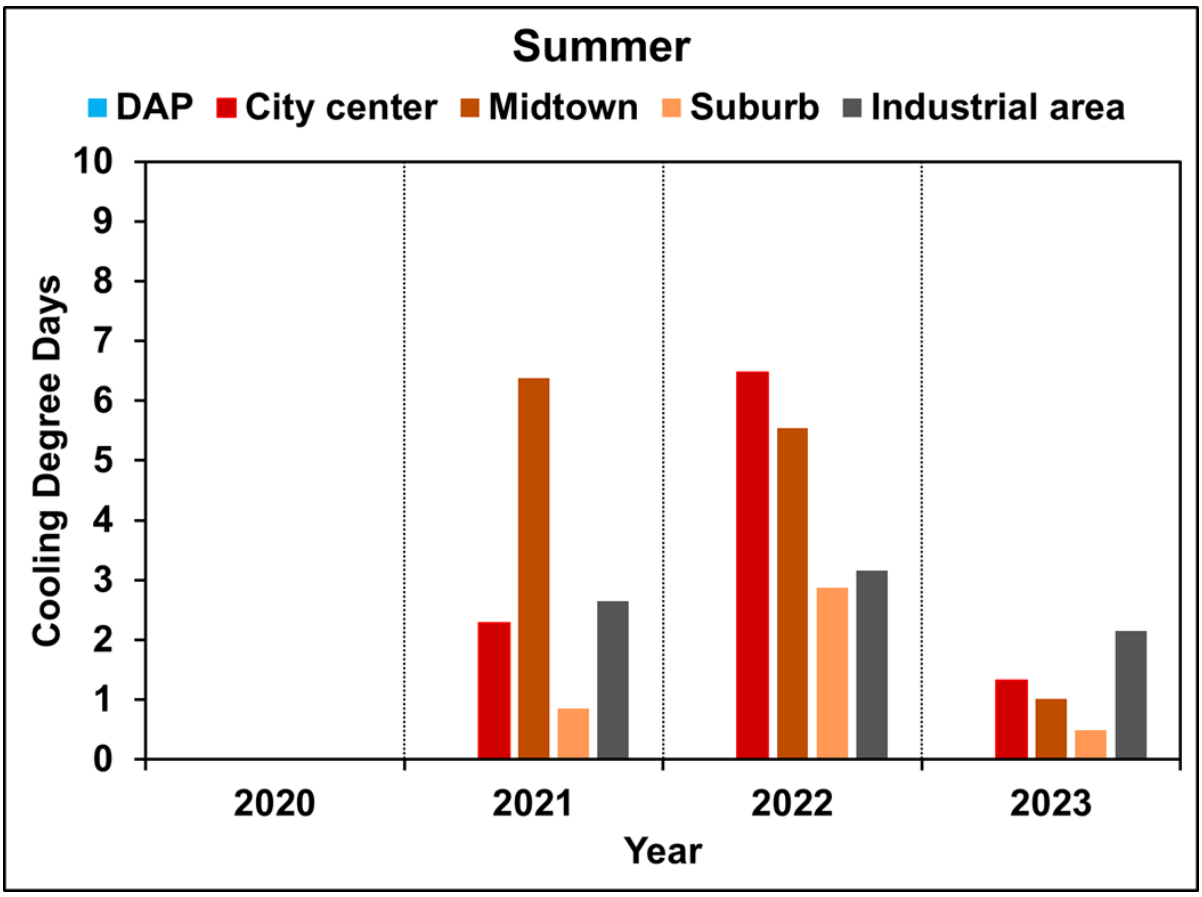

Figure 29: Comparison of CDD for the summer season between the LCZs and Dublin Airport (DAP). The CDD are zero for all four years at DAP.

The low number of CDD reflects that Dublin doesn't have a high energy demand for cooling the city. To examine the heating demand, we have also analysed the HDD for the winter season of the four years. An HDD is said to occur when the outside temperature is cold enough to require heating inside (i.e. in a building/dwelling) and is calculated as the difference between the threshold value and the mean temperature of a day. The comparison of HDD between LCZs and DAP in figure 30 show the large number of HDD occurrence in the winter. Again, there is a clear difference between the values at the airport and the residential areas, and the values are almost always higher at the DAP by 50 -100 HDD. The figure reflects that the residential areas might need lower heating energy demands and the calculations/policies from DAP could be misleading to higher values. The energy distribution policies should include these differences in the residential areas to avoid any energy losses related to the oversupply in the winter months.

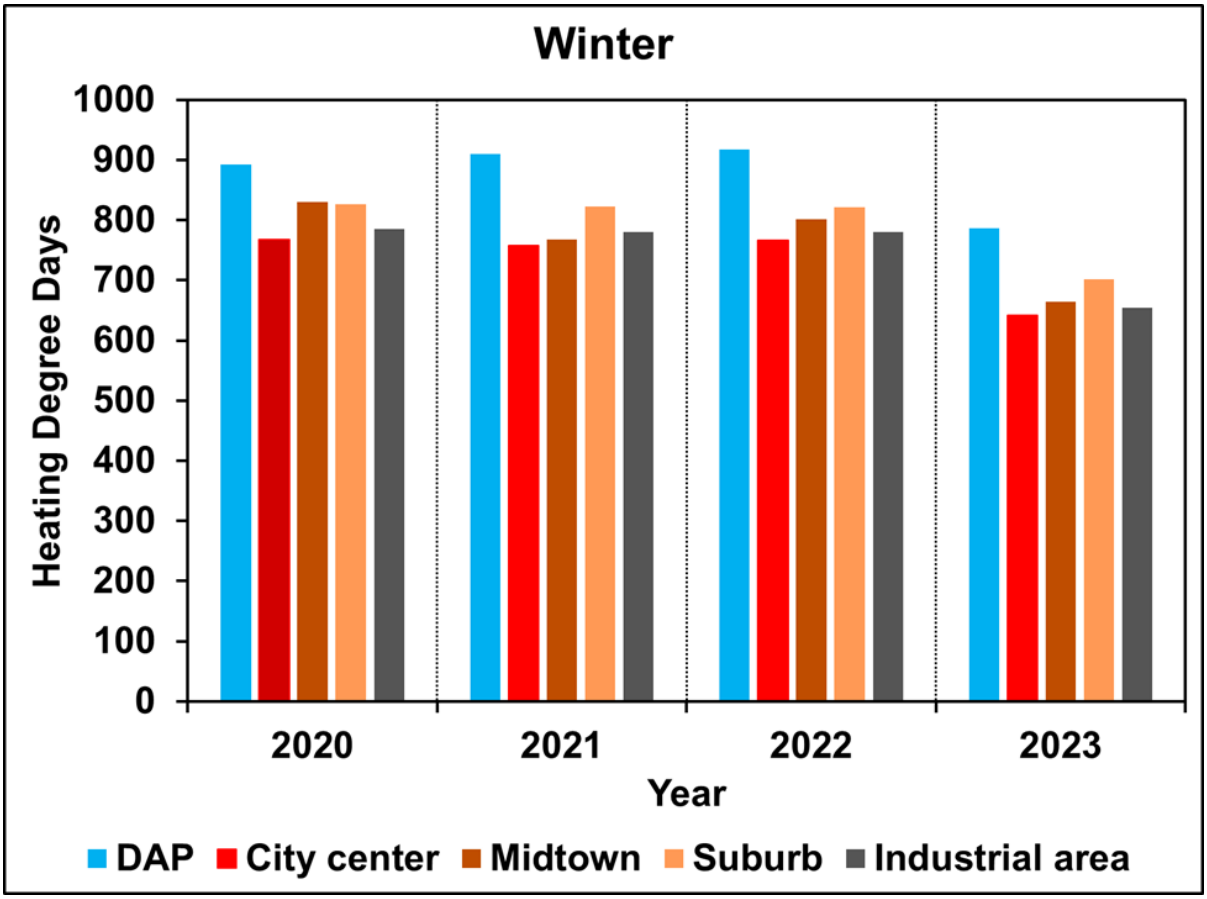

Figure 30: Comparison of HDD for the winter season between the LCZs and DAP

5.2 Climate change and degree days

The high-resolution climate projections by Nolan (2024) indicates that the mean annual 2m temperature over Ireland is projected to increase by 0.5–3°C depending on time-period and future climate scenarios. The projected increases in temperature around Dublin areas for summer season are up to 3.0°C in for high emission scenarios (HES: 2071–2100) and by 1 C for low emission scenarios (LES: 2021-2050). Similarly. The increase values are about 0.7 C (2.) C) in Low (high) emission scenarios for winter season. We project seasonal values from 2023 for both emission scenarios listed in Table 6. There is a clear indication of the increase in the CDD for the HES and decrease in HDD for winter in both scenarios. Our results echo the findings of Buckley et al., (2021) where they reported 1-3 days increase of CDD by 2050 and a great reduction in HDD days. They projected that the impact of climate change for Dublin will be to reduce the annual residential heating demand and a marginal impact on cooling demand. These

projections also reflect the necessity of separating the residential areas and the DAP to have effective energy supply policies.

Table 6: Current and projected cooling and heating degree days for different emission scenarios

Cooling Degree days					
	Dublin Airport	**City center**	**Midtown**	**Suburb**	**Industrial Areas**
Current (2023)	0	1.3	1.0	0.5	2.3
LES 2021-2050	0	1.6	1.3	1.0	4.0
HES 2071-2100	2.2	10.8	5.7	4.3	14.2
Heating Degree Days					
	Dublin Airport	**City center**	**Midtown**	**Suburb**	**Industrial Areas**
Current (2023)	786	642	648	702	655
LES 2021-2050	722	530	544	588	543
HES 2071-2100	543	186	197	232	133

5.3 Heat Stress

Climate projections for Ireland suggest that average summer temperatures will rise by 1–3 °C by 2100, accompanied by more frequent and intense hot spells. These changes are expected to increase heat-related health risks, particularly among older adults and socially isolated individuals. The Urban Heat Island (UHI) effect will amplify these risks by raising nighttime temperatures and reducing recovery periods during prolonged heat events. In Dublin, the UHI effect means that city temperatures remain several degrees higher than in reference station Pheonix park, especially at night. This is driven by dense built infrastructure, limited vegetation, and anthropogenic heat release. During heat waves, UHI intensifies health impacts by further reducing nighttime cooling. Evidence shows that UHI hotspots in Dublin are closely linked to higher vulnerability, particularly in densely populated and deprived neighbourhoods (Pascal, 2011).

A 2021 study conducted by Paranunzio et al. (2021) introduced an extreme heat stress risk index specifically for Dublin city, projecting changes through the 2020s to the 2050s. Using a combination of LCZ and UHI and spatially explicit socioeconomic indicators, the study produced a fine-scale map of heat hazard, vulnerability, and overall heat risk. The findings indicate that urban areas classified as highest risk are expected to increase by approximately 70% under LES and by a striking 96% under HES between the 2020s and 2050s. Particularly elevated heat risk is projected in Dublin's core city center and its northern and western districts under the more extreme scenario (RCP 8.5)

5.4 Policy recommendations

The findings from the summertime Urban Heat Island (UHI) analysis for Dublin (2020–2023) provide a strong empirical basis for targeted policy interventions to mitigate UHI impacts, improve urban liveability, and enhance climate resilience. The recommendations below are structured around four key thematic areas: urban planning and design, climate adaptation and public health, energy and environmental policy, and monitoring and modelling frameworks.

Action 1: Enhance Monitoring and Data Capacity for Policy Integration

1.1 Monitoring, Modelling, and Data Integration:

- The current Community Weather Station (CWS) network provides valuable insights but remains spatially limited. Expand the urban meteorological network with denser sensor coverage across LCZs. This will insure that policy actions and measures are evidence based and focused, and as they are implemented monitor the effectiveness of the interventions.

1.2 Refinement of Degree-Day Metrics

Current Cooling Degree Day (CDD) and Heating Degree Day (HDD) values derived from Dublin Airport (DAP) are not representative of residential temperature conditions within the city.

- Calculate degree days using area-based observations (especially midtown and suburbs) to more accurately assess urban energy demand.
- Adjust energy supply planning and efficiency targets to reflect real urban temperature profiles, avoiding overestimation of winter heating needs.
- Encouragement of Passive and Renewable Cooling Systems

Action 2: Urban Planning and Design

Note: Local Authorities will be producing new development plans commencing in 2026 this is an opportunity to strengthen existing actions within these plans, to ensure that planning enable climate resilience. For example, within Dublin City Council's Development Plan 2022-2028 Chapter 15 addresses development standards, as they relate to climate mitigation and adaptation. This research further strengthen the necessity implementing and enforcing requirements for nature based solutions.

2.1 Integrating Local Climate Zones (LCZ) into Urban Planning:

- Urban design guidelines should incorporate microclimatic performance criteria, linking building form, material selection, and vegetation coverage to UHI mitigation outcomes. This will ensure that development is climate proofed.

2.2 Green and Blue Infrastructure expansion:

Significant work has been done to date by Local Authorities on

- Expansion of urban green networks through improved connectivity between parklands, street trees, and linear green corridors to diffuse cooling into adjacent neighbourhoods to create green necklaces and biodiversity corridors
- Encourage the implementation of green roofs, green façades, and pocket parks particularly in dense built-up LCZs (city center, midtown) by making these conditions of planning and through changes in building regulations (see Action 3.2).
- Protect and enhance urban waterways, rivers, ponds, lakes and wetlands to exploit evaporative cooling effects.

- Integrate nature based solutions into playgrounds to insure spaces can serve as a cooling space.

2.3 Industrial Zone Heat Management:

- Industrial areas (LCZ 8 & 10) exhibit secondary UHI peaks due to extensive paved surfaces, low vegetation, and heat emissions from industrial activity.
- Incorporate heat emission limits and waste heat recovery requirements within industrial permitting processes.
- Implement vegetated buffers and shade trees in and around industrial estates.
- Encourage the installation of cool roof systems and permeable surfacing in logistics and manufacturing sites.
- For workers based at industrial sites provide training in identifying signs of heat related illnesses and responding.

Action 3: Climate Adaptation and Public Health

3.1 Development of an Urban Heat Action Plan (UHAP):

Given the amplification of heat stress during anticyclonic (fair-weather) conditions, Dublin requires a comprehensive Urban Heat Action Plan (UHAP).

- Integrate UHI data with National Climate Change Risk Assessment to support development of Urban Heat Action Plan.
- Designate “cooling centres” in community centres, libraries, sports facilities, and schools for vulnerable populations during heatwaves.

3.2 Climate-Resilient Building and Design Standards:

Projected warming (+1 to +3°C by 2100) necessitates adaptation in the built environment.

- Revise building regulations to promote passive cooling, shading, ventilation crossflows, and thermal insulation that minimizes indoor overheating.
- Encourage green retrofitting programmes in older residential areas within LCZs 2–5 to reduce heat stress during extreme events.
- Expand existing retrofit programmes to provide grant support for climate resilient retrofits, with a specific focus on nature based solutions interventions (ie. Rainwater planters, de paving of driveways, planting of drought resistant flora)

3.3 Targeted Heat-Health and Social Measures – Just Resilience:

The intersection of UHI hotspots and social vulnerability increases health risks during heat events. Research highlights that in areas of social deprivation, antisocial behaviour increases during heat events, reducing this risk needs considered and tailored action.

- Implement targeted public health interventions in high-risk districts (northern and western inner-city areas). That consider the local context in terms of a socio economic status, gender profile and race
- Increase awareness of UHI exposure risks as identified in the Health Sectoral Adaptation Plan and embed in Health Service Executive (HSE) public health and emergency preparedness plans.
- Partner with community groups to deliver heat awareness and hydration campaigns during forecasted hot spells.
- Establish a programme with community groups to check on vulnerable people during heat events.
- Work with local area offices to develop programme of activities that reduce risk of anti social behavior.

3.4 Working conditions

Temperature is a challenge for workers. A recent report by the International Labour Organisation (ILO) highlights the hazards posed by exposure to heat, UV radiation, and air pollution. These risks need to be considered by all levels of government

- Assess current health and safety practices for indoor and outdoor workers in relation to heat and develop protocols
- For outdoor workers provide training for identification of heat related illnesses
- Employers should insure out door workers have access to cooling spaces.

6 Conclusions

This report provides a comprehensive framework for understanding UHI dynamics through a synergistic approach combining citizen science, climatological analysis, and advanced numerical modelling. The insights are directly relevant for urban planners, policymakers, health experts, energy providers, and researchers aiming to adapt to a warming urban future.

Despite its obvious advantages and its potential, the crowdsourced meteorological data derived from unconventional sources like the AWS networks cannot be considered scientifically adequate without satisfactory quality control. Hence the applicability and performance of such data in the study of urban climates are nearly entirely reliant on the success of the employed quality assurance methods. Present study deliberately applied the simplest possible quality control and quality assurance methods to achieve a robust enough data set for the further study of the urban climate of Dublin and evaluate the applicability and performance of crowdsourced meteorological data in different temporal resolution.

The UHI effect in Dublin is most prominent during summer nights (June to August), with average nighttime UHI intensities reaching up to 4.3°C and peaking at around 5.5°C in denser urban zones (e.g., city center and midtown). Spatial maps of UHI intensity reveal that the highest temperature anomalies are in the city centre and industrial estates, while parks and coastal zones exhibit cooler conditions. Temporal analysis confirms that UHI peaks after sunset and sustains until early morning, collapsing at sunrise due to boundary layer mixing. The canopy layer UHI analysis is complemented by daytime surface UHI derived from ECOSTRESS and night-time surface UHI from the MODIS Aqua product which exhibit the similar urban-rural patterns.

Analysis by LCZ demonstrated the role of urban morphology in influencing thermal behaviour. Densely built zones exhibited higher nocturnal UHI, while open low-rise and green suburban areas cooled faster and had significantly lower UHI intensities. Industrial zones (LCZ10) also displayed elevated nighttime UHI due to retained and generated heat. The summertime Urban Heat Island (UHI) analysis for Dublin (2020–2023) reveals that urban areas, particularly the city centre and midtown zones, experience significantly higher nighttime temperatures than surrounding suburbs, highlighting the need for targeted mitigation and adaptation measures. The findings support a coordinated policy approach centred on four key areas:

- enhancing monitoring and modelling capacity by expanding Dublin’s meteorological network for more accurate, spatially resolved data.
- Integrate "Heat Zoning" into Planning to promote climate-sensitive design and expand green and blue infrastructure.
- strengthening climate adaptation and public health measures through an Urban Heat Action Plan, improved building standards, and targeted support for vulnerable populations and outdoor workers. refining energy and climate policies by using localized temperature data to improve energy efficiency and promote passive cooling systems.

Collectively, these actions aim to reduce heat exposure, enhance urban resilience, and improve overall liveability under a warming climate.

References

Alexander, P. and Mills G. (2014) 'Local climate classification and Dublin's urban heat island'. Atmosphere, 5. pp.755-774

Anser, M. K., Nassani, A. A., Al-Aiban, K. M., Zaman, K., & Haffar, M. (2025). Urban heat islands and energy consumption patterns: Evaluating renewable energy strategies for a sustainable future. Energy Reports, 13, 3760–3772. https://doi.org/10.1016/j.egyr.2025.03.033

AppEEARS Team. (2026). Application for Extracting and Exploring Analysis Ready Samples (AppEEARS). Ver. 3.115. NASA EOSDIS Land Processes Distributed Active Archive Center (LP DAAC), USGS/Earth Resources Observation and Science (EROS) Center, Sioux Falls, South Dakota, USA. Accessed April 10, 2026. https://appeears.earthdatacloud.nasa.gov

Baki, H., Chinta, S., C Balaji, and Srinivasan, B.: Determining the sensitive parameters of the Weather Research and Forecasting (WRF) model for the simulation of tropical cyclones in the Bay of Bengal using global sensitivity analysis and machine learning, (2022) Geosci. Model Dev., 15, 2133–2155, https://doi.org/10.5194/gmd-15-2133-2022.

Basara, J.B. et al. (2011) 'The Oklahoma City Micronet'. Meteorological Applications, 18(3). Pp.252-261

Bechtel, B. et al., (2015). Mapping Local Climate Zones for a Worldwide Database of the Form and Function of Cities. ISPRS International Journal of Geo-Information, 4(1), 199-219. https://doi.org/10.3390/ijgi4010199

Beele, E., Reyniers, M., Aerts, R., and Somers, B (2022): Quality control and correction method for air temperature data from a citizen science weather station network in Leuven, Belgium, Earth Syst. Sci. Data, 14, 4681–4717, https://doi.org/10.5194/essd-14-4681-2022

Büchau, Y. G. (2018). Modelling Shielded Temperature Sensors. An Assessment of the Netatmo Citizen Weather Station. [Master's thesis, University of Hamburg]. https://bis-erdsystem.de/fileadmin/user_upload/bise/ Texte/MSC_Met_61-20180313.pdf

Buckley, N.; Mills, G.; Letellier-Duchesne, S.; Benis, K. (2021). Designing an Energy-Resilient Neighbourhood Using an Urban Building Energy Model. Energies 14, 4445. https://doi.org/10.3390/en14154445

Chandler, T.J. (1965). The Climate of London (1st ed.). Routledge. https://doi.org/10.4324/978100363446

Chapman, L. (2015) 'Urban Meteorological Networks: an urban climatologist's panacea?'. International Association for Urban Climate, 58(12). pp.7-12

Chapman, L. et al. (2015) 'The Birmingham Urban Climate Laboratory'. Bulletin of the American Meteorological Society, 96(9). pp.1545-1560

Chapman, L.; et al., (2017) 'Can the crowdsourcing data paradigm take atmospheric science to a new level? A case study of the urban heat island of London quantified using Netatmo weather stations. International Journal of Climatology, 37(9). pp.3597-3605

Coney, J., Pickering, B., Dufton, D., Lukach, M., Brooks, B., & Neely III, R. R. (2022). How useful are crowdsourced air temperature observations? An assessment of Netatmo stations and quality control schemes over the United Kingdom. Meteorological Applications, 29(3), e2075. https://doi.org/10.1002/met.2075

de Bode, M., Hedde, T., Roubin, P., &Durand, P. (2023). A method to improve land use representation for weather simulations based on high-resolution datasets—Application to Corine Land Cover data in the WRF model. Earth and Space Science, 10, e2021EA002123.

Demuzere M., Arguesso D., Zonat A. and Kitter J., (2022). W2W: A Python package that injects WUDAPT's Local Climate Zone information in WRF. Journal of Open-Source Software, 7(76), 4432. https://doi.org/10.21105/joss.04432

Demuzere, M., Kittner, J., & Bechtel, B. (2021). LCZ Generator: A Web Application to Create Local Climate Zone Maps. Frontiers in Environmental Science, 9. https://www.frontiersin.org/articles/10.3389/fenvs.2021.63 7455

Dickinson, J.L., Zuckerberg, B. and Bonter, D.N. (2010) 'Citizen science as an ecological research tool: challenges and benefits. Annual Review of Ecology, Evolution, and Systematics. 41. pp.149-172

Fealy, R., and Mills. G. (2018). Deriving Lamb weather types suited to regional climate studies: a case study on the synoptic origins of precipitation over Ireland. Int. J. Climatol., 38, 3439-3448, 10.1002/joc.5495

Fenner, D., Bechtel, B., Demuzere, M., Kittner, J., & Meier, F. (2021). CrowdQC+—A Quality Control for Crowdsourced Air-Temperature Observations Enabling World-Wide Urban Climate Applications. Frontiers in Environmental Science, 9. https://doi.org/10.3389/fenvs.2021.720747

Ferster C. et al. (2017) 'Promoting Crowdsourcing for urban research: cycling safety citizen science in four cities. Urban Science, 1(2). pp.1-17

Graham, E. (1993) 'The urban heat island of Dublin city during summer months. Irish Geography, 26(1). pp.45-57

Gülch, E., Uddin, S. and Willi, B. (2016) 'Beesmart – A crowdsourcing project with smartphones. The International Archives of the Photogrammetry, Remote Sensing and Spatial Information Sciences, XLI-B3. pp.863-870

Hahn, C., Garcia-Marti, I., et al. (2022). Observations from Personal Weather Stations—EUMETNET Interests and Experience. Climate, 10(12), 192. https://doi.org/10.3390/cli10120192

Haughey E. (2021). Climate Change and Land Use in Ireland. EPA Report No. 371. DOI:10.13140/RG.2.2.20273.30568

Hook, S., & Hulley, G. (2022). ECOSTRESS Tiled Land Surface Temperature and Emissivity Instantaneous L2 Global 70 m v002. NASA Land Processes Distributed Active Archive Center. https://doi.org/10.5067/ECOSTRESS/ECO_L2T_LSTE.002. Accessed April 10, 2026.

Jones, P.D., Harpham, C. and Briffa, K.R. (2013) Lamb weather types derived from reanalysis products. International Journal of Climatology, 33, 1129–1139. https://doi.org/10.1002/joc.3498

Kittner, J., Demuzere, M., & Bechtel, B. (2021). Crowdsourcing von Lufttemperaturmessdaten zur kleinräumigen Modellierung von städtischen Temperaturverteilungen.

Kolokotorni, M., Ren, X., Davies, M. and Mavrogianni, A. (2012) 'London's urban heat island: Impact on current and future energy consumption in office buildings. Energy and Buildings, 47. pp.302-311

Koskinen, J.T. et al. (2011) 'The Helsinki testbed: A mesoscale measurement, research, and service platform'. Bulletin of the American Meteorological Society, 92(3). pp.325-342

Krelaus, L., Apfel, J., Bechtel, B., & Sismanidis, P. (2023). Surface and canopy-layer urban heat island intensities in Europe – Quantifying differences in the diurnal cycle for three summer periods. 2023 Joint Urban Remote Sensing Event (JURSE), 1–4. https://doi.org/10.1109/JURSE57346.2023.10144174

Laaidi, K. et al. (2012) 'The Impact of Heat Islands on Mortality in Paris during the August 2003 Heat Wave'. Environmental Health Perspectives, 120(2). pp. 254-259

Levermore, G., Parkinson, J, Kwanho, L. and Laycock, P. (2018) 'The increasing trend of the urban heat island intensity'. Urban Climate, 24(6). pp.360-368

Li S.H., Sifton, V., Lundgren, J., McClellan, C. and Gibbons, M. (2021) Extreme wind climate of the Arabian Peninsula characterized by using WRF simulation, Weather and Climate Extremes,33,100330, https://doi.org/10.1016/j.wace.2021.100330

Li, X., Zhou, Y., Yu, S., Jia, G., Li, H., & Li, W. (2019). Urban heat island impacts on building energy consumption: A review of approaches and findings. Energy, 174, 407–419. https://doi.org/10.1016/j.energy.2019.02.183

Mandement, M., & Caumont, O. (2020). Contribution of personal weather stations to the observation of deep-convection features near the ground. Natural Hazards and Earth System Sciences, 20(1), 299–322. https://doi.org/10.5194/nhess-20-299-2020

Meier, F. et al. (2017) 'Crowdsourcing temperature from citizen weather stations for urban climate research'. Urban Climates, 19. pp.170-191

Met Éireann (2020). https://www.met.ie/climate/climate-of-ireland.Accessed on 07.05.2025

Mohan, M., Sati, A. P., and Bhati, S. (2020) Urban sprawl during five decadal period over National Capital Region of India: Impact on urban heat island and thermal comfort, Urban Climate,33, 100647, https://doi.org/10.1016/j.uclim.2020.100647

Muller, C.L. et al. (2013) 'Sensors and the city: a review of urban meteorological networks. International Journal of Climatology, 33(7). pp.1585-1600

Naserikia, M., Hart, M. A., Nazarian, N., Bechtel, B., Lipson, M., & Nice, K. A. (2023). Land surface and air temperature dynamics: The role of urban form and seasonality. Science of The Total Environment, 167306. https://doi.org/10.1016/j.scitotenv.2023.167306

Oke, T.R. (1982) 'The energetic basis of the urban heat island'. Quarterly Journal of the Royal Meteorological Society, 108. pp.1-24

Oke, T.R., Mills, G., Christen, A. and Voogt, J.A. (2017) 'Urban climates. Cambridge: Cambridge University Press

Overeem, A. et al. (2013) 'Crowdsourcing urban air temperatures from smartphone battery temperatures. Geophysical Research Letters, 40(15). pp.4081-4085.

Paranunzio, R., Dwyer, E., Fitton, J. M., Alexander, P. J., & O'Dwyer, B. (2021). Assessing current and future heat risk in Dublin city, Ireland. Urban Climate, 40, 100983. https://doi.org/10.1016/j.uclim.2021.100983

Pascal, M. (2011). An Analysis of the Mortality Risks Associated with Heat and Heat Waves in Ireland, toAssist in Planning for Climate Change. Doctoral Thesis. Technological University Dublin. doi:10.21427/D7R302

Rajapaksha, T.T., Alexander, A., Fernando, L. et al. (2022). Real-Time Weather Monitoring and IoT-Based Palmtop Device for Smart Agriculture. SN COMPUT. SCI. 3, 91. https://doi.org/10.1007/s42979-021-00961-6

Rendfrey, T.S., Bukovsky, M. S., McCrary, R.R., and Fuentes-Franco, R. (2021) An assessment of tropical cyclones in North American CORDEX WRF simulations, Weather and Climate Extremes,34, 100382, https://doi.org/10.1016/j.wace.2021.100382

Roberts, H., Sadler, J. and Chapman, L. (2017) 'Using Twitter to investigate seasonal variation in physical activity in urban green space'. Geo: Geography and Environment, 4(2), pp.1-14

Santamouris, M. (2014) 'On the energy impact of urban heat island and global warming on buildings. Energy and Buildings, 82. pp.100-113

Stewart, I.D. (2011) 'A systematic review and scientific critique of methodology in modern urban heat island literature'. International Journal of Climatology, 31(2). pp.200-217

Sweeney, J.C. (1987) 'The urban heat island of Dublin city'. Irish Geography, 20(1). pp.1-10

Taha, H. (1997) 'Urban climates and heat islands: albedo, evapotranspiration, and anthropogenic heat'. Energy and Buildings, 25. pp.99-103

Vuckovic, M., & Schmidt, J. (2023). On the Importance of Data Quality Assessment of Crowdsourced Meteorological Data. Sustainability, 15(8), 6941. https://doi.org/10.3390/su15086941

Wan, Z., Hook, S., & Hulley, G. (2021). MODIS/Aqua Land Surface Temperature/Emissivity 8-Day L3 Global 1km SIN Grid V061. NASA Land Processes Distributed Active Archive Center. https://doi.org/10.5067/MODIS/MYD11A2.061.

Warren, E.L. et al. (2016) 'The Birmingham urban Climate laboratory – A high density, urban meteorological dataset, from 2012-2014. Scientific Data, 3(6).

Williams, M. et al. (2011) 'Automatic processing, quality assurance and serving of real-time weather data'. Computers and Geosciences, 37(3). pp.353-362

Yang, P. and Ng, T.L. (2017) 'Gauging Through the Crowd: A Crowd-Sourcing Approach to Urban Rainfall Measurement and Storm Water Modeling Implications'. Water Resources Research, 53(11). pp.9462-9478

Yang, T., Li, Q., Hamdi, R., et al., (2022). Snowfall climatology in the Tianshan Mountains based on 36 cold seasons of WRF dynamical downscaling simulation, 270, 106057, https://doi.org/10.1016/j.atmosres.2022.106057

Young, D.T. et al. (2014) 'A low-cost wireless temperature sensor: evaluation for use in environmental monitoring applications. Journal of Atmospheric and Oceanic Technology, 31(4). pp.938-944

Appendix A: Station Details

Table A1 provides the location, data start date and the variables recorded at the tree met station used in the report viz., Casement, Dublin Airport and Phoenix park.

Table A1: Details of the three met stations around Dublin

	Dublin Airport	Phoenix Park	Casement
Location	Latitude:53.428 Longitude: -6.241 Station Height: 71 M	Latitude: 53.364 Longitude: -6.350 Station Height: 48 M	Latitude:53.306 Longitude: -6.439 Station Height: 91 M
Data from	January 1945	August 2003	January 1964
Variables recorded	• Precipitation Amount (mm) • Air Temperature (C) • Wet Bulb Temperature (C) • Dew Point Temperature (C) • Relative Humidity (%) • Vapour Pressure (hPa) • Mean Sea Level Pressure (hPa) • wdsp: - Mean Wind Speed (knot) • wddir: - Predominant Wind Direction (degree) • Synop code for Present Weather • Synop code for Past Weather • Sunshine duration (hours) • Visibility (m) • Cloud height (100's of ft) • Cloud amount	• Precipitation Amount (mm) • Air Temperature (C) Wet Bulb Temperature (C) • Dew Point Temperature (C) • Vapour Pressure (hPa) • Relative Humidity (%) • Mean Sea Level Pressure (hPa)	• Precipitation Amount (mm) • Air Temperature (C) • Wet Bulb Temperature (C) • Dew Point Temperature (C) • Relative Humidity (%) • Vapour Pressure (hPa) • Mean Sea Level Pressure (hPa) • wdsp: - Mean Wind Speed (knot) • wddir: - Predominant Wind Direction (degree) • Synop code for Present Weather • Synop code for Past Weather • Sunshine duration (hours) • Visibility (m) • Cloud height (100's of ft) Cloud amount

Table A1 provides details of the CWS stations located within Dublin city. As noted in the section 2.2, these stations have varying start and end dates. The table also highlights in red the stations that were excluded from the current analysis due to insufficient data, either because they operated only for a short period or contained large gaps in the recorded data.

Table A2: The location, local climate classification of the various CWS stations.

intern_id	lat	lon	altitude	lcz
intern_117822	53.18179	-6.16452	117	11
intern_117824	53.20172	-6.12808	16	6
intern_117825	53.22633	-6.13468	43	12
intern_117826	53.25567	-6.21792	131	6
intern_117830	53.26196	-6.20739	101	6

intern_117835	53.2817	-6.24262	75	5
intern_117836	53.28641	-6.24949	70	6
intern_117838	53.27874	-6.21672	89	8
intern_117843	53.27549	-6.10702		6
intern_117850	53.28917	-6.28895	62	6
intern_117853	53.30926	-6.24557	30	6
intern_117857	53.31277	-6.20649	11	4
intern_117858	53.30902	-6.20606	12	6
intern_117862	53.2907	-6.20662	64	6
intern_117867	53.29967	-6.18114	19	5
intern_117869	53.29563	-6.13791	32	4
intern_117874	53.31847	-6.28673	35	6
intern_117881	53.3418	-6.43168	57	6
intern_117885	53.33784	-6.2756	17	2
intern_117893	53.33868	-6.24866	18	2
intern_117895	53.33808	-6.23571	2	4
intern_117901	53.36236	-6.51618	55	6
intern_117902	53.36857	-6.492	37	6
intern_117912	53.36517	-6.20023	14	6
intern_117913	53.37493	-6.19408	28	6
intern_117914	53.37798	-6.15987	9	6
intern_117919	53.39106	-6.18759	30	6
intern_117921	53.39855	-6.43948	64	6
intern_117922	53.39829	-6.42864	59	6
intern_117925	53.40359	-6.39579	56	6
intern_117927	53.39928	-6.25506	60	5
intern_117929	53.42503	-6.13717	2	6
intern_123334	53.29604	-6.14179	17	4
intern_123336	53.33541	-6.54954	62	6
intern_123338	53.39435	-6.3015	67	8
intern_125854	53.40505	-6.16781	3	8
intern_128993	53.32004	-6.27413	30	6
intern_128994	53.32376	-6.23808	12	6
intern_151506	53.2661	-6.22143	131	6
intern_153197	53.29594	-6.2035	34	6
intern_156473	53.44404	-6.13472	23	6
intern_156917	53.28508	-6.16063	40	6
intern_159648	53.4533	-6.17255	9	6
intern_162503	53.26592	-6.21958	124	6
intern_164809	53.14646	-6.0718	19	6
intern_173472	53.31891	-6.24923	24	6
intern_173889	53.29723	-6.27884	51	6
intern_175524	53.35265	-6.4213	51	6
intern_176730	53.39238	-6.42778	59	6
intern_177811	53.32345	-6.38388	54	6
intern_180269	53.35221	-6.23435	3	4

intern_193850	53.36391	-6.24645	3	5
intern_200292	53.40442	-6.16638	15	8
intern_204409	53.29448	-6.13625	13	10
intern_208179	53.38911	-6.42625	60	6
intern_208918	53.36035	-6.50681	53	12
intern_210459	53.39787	-6.40376	59	6
intern_215208	53.25233	-6.11648	29	6
intern_216740	53.28266	-6.14511	40	4
intern_217058	53.3379	-6.2591	14	12
intern_217712	53.45171	-6.19757	16	6
intern_223061	53.26534	-6.21975	126	6
intern_223703	53.29297	-6.24971	48	6
intern_230765	53.34294	-6.24454	5	10
intern_233742	53.30734	-6.28137	46	6
intern_234992	53.40069	-6.15399	12	5
intern_247937	53.1304	-6.0755	34	6
intern_247943	53.27254	-6.09885	68	6
intern_247944	53.34665	-6.31099	3	6
intern_247946	53.3382	-6.2591	14	12
intern_247948	53.36235	-6.3048	39	6
intern_247949	53.40591	-6.15277	5	8
intern_247950	53.42555	-6.1347	4	6
intern_249873	53.27598	-6.17963	82	6
intern_251131	53.27451	-6.13338	49	6
intern_255697	53.22126	-6.23177	300	14
intern_257248	53.38136	-6.16825	17	6
intern_259044	53.30832	-6.26866	41	6
intern_267828	53.44593	-6.20044	21	6
intern_273793	53.26373	-6.16179	49	6
intern_275111	53.29517	-6.19062	35	6
intern_277119	53.30612	-6.29093	47	6
intern_277120	53.30563	-6.23971	32	6
intern_277121	53.38861	-6.07359	7	12
intern_280794	53.3037	-6.1831	15	
intern_280795	53.36756	-6.18815	16	6
intern_282927	53.33945	-6.558	62	12
intern_283680	53.2851	-6.22921	76	6
intern_284045	53.28537	-6.14134	34	5
intern_284046	53.38333	-6.28781	47	6
intern_284320	53.32256	-6.24728	16	5
intern_286695	53.38777	-6.07156	21	6
intern_290525	53.3297	-6.2708	20	6
intern_295087	53.34147	-6.41518	58	6
intern_295647	53.33151	-6.23239	7	4
intern_296121	53.28614	-6.14068	35	6
intern_296892	53.37999	-6.28934	32	6

intern_300213	53.29435	-6.15457	16	6
intern_302458	53.39285	-6.25868	56	6
intern_302665	53.323	-6.3159	47	12
intern_303410	53.25678	-6.11458	30	6
intern_303787	53.3627	-6.26111	12	6
intern_305222	53.15683	-6.18603	246	9
intern_307059	53.3339	-6.2271	8	4
intern_307493	53.39375	-6.24277	55	6
intern_309767	53.2963	-6.1304	5	
intern_309768	53.3334	-6.23735	7	5
intern_310295	53.29032	-6.17627	30	6
intern_311045	53.33062	-6.21277	3	6
intern_314415	53.30945	-6.20364	10	6
intern_315097	53.13884	-6.09153	75	9
intern_315098	53.30488	-6.23785	36	6
intern_318042	53.40097	-6.1442	4	6
intern_320382	53.36361	-6.27961	30	6
intern_320531	53.33957	-6.21743	4	8
intern_323408	53.37493	-6.19408	28	6
intern_323918	53.27035	-6.22986	106	6
intern_326148	53.25076	-6.19892	108	14
intern_326820	53.35074	-6.4314	47	6
intern_327066	53.26413	-6.22479	129	6
intern_327947	53.42503	-6.13717	2	6
intern_328083	53.323	-6.3159	41	12
intern_328580	53.12397	-6.07597	45	6

Appendix B: WRF Modelling Details

B.2 Model Description

The details of the WRF model are given in the user's guide (Michalakes et al., 2004; Skamarock et al., 2021) and a summary is presented here. The Advanced Research WRF (ARW) modelling system is a continuously evolving and developing development for last couple of decades. The ARW is a flexible, efficient, state-of-the-art atmospheric simulation system on various parallel computing platforms. It is suitable for use in a broad range of applications across scales ranging from few meters to thousands of kilometres, for research in parameterization, data assimilation, forecast and real-time predictions, regional climate studies etc. The schematic of WRF model is shown in Figure B1 with the two main components WRF Preprocessing System (WPS) and the ARW solver. Additionally, there are several post processing graphic tools to analyse the model outputs.

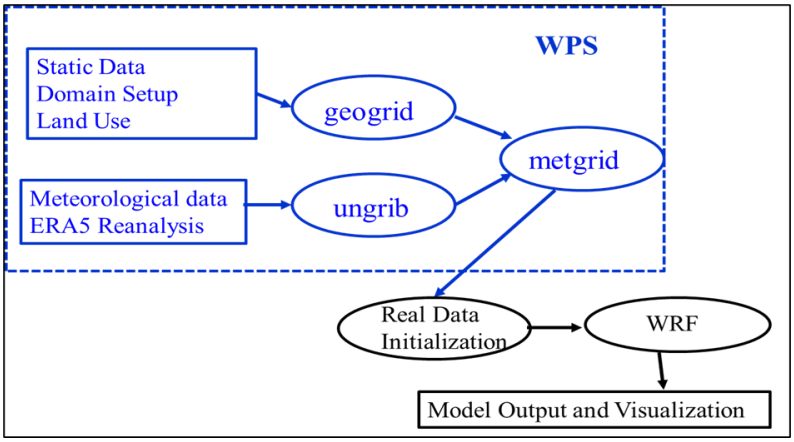

Figure B1: Schematic of the Model Set-up showing intermediate steps for model simulation

B.3 Simulation details

The model simulation is for May 2020 when the UHI is highest in that year. The WRF model was run for 31 days from 1st to 31st May 2020. Most of the WRF based studies take only 12-24 h of spin up duration (Sati and Mohan 2018; Segura et al., 2021). In the present work too, we have taken 48 h as a suitable spin up duration for our model setup.

B.3.1 Synoptic conditions

May 2020 was another very dry and settled month with a dominating high-pressure system. The high pressure was in the northwest of Ireland in the first half while in the second half of the month it positioned to the south of the country, which brought a milder airflow from the southwest. Between the 21st and 23rd, the remnants of post-tropical storm Arthur came close to the west coast of Ireland which brought widespread rain, heaviest in the southwest, and the strongest winds of the month. The weather settled down again from the 24th with high-pressure building from the south and drifting over Ireland towards Scandinavia, keeping it mostly dry and very warm up to the end of the month. The rainfall was below average, drier in the eastern half of the country while the temperatures and sunshine hours were above average across the Island (Met Éireann reports).

B.3.2 Domain setup

ARW provides the capability to focus on the study region which can be 1-way or 2-way nesting options. We have set-up the WRF Model Figure B2) for double nested domain with the entire country of Ireland as inner domain. We used the nesting grid ratio of 1:10 and the horizontal grid spacing of the inner, and outer domain is 1 km, and 10 km respectively with 1-way nesting. In both 1-way and 2-way simulation modes, the fine-grid (inner) boundary conditions are interpolated from the coarse-grid (outer) domain. The difference in 1 way nest is that in the information exchange is only from the coarse grid to the fine grid (Skamarock et al., 2021; Michalakes et al., 2004). As a general guideline, the Lambert conformal projection is well-suited for mid-latitude domains which we deem suitable for our domain.

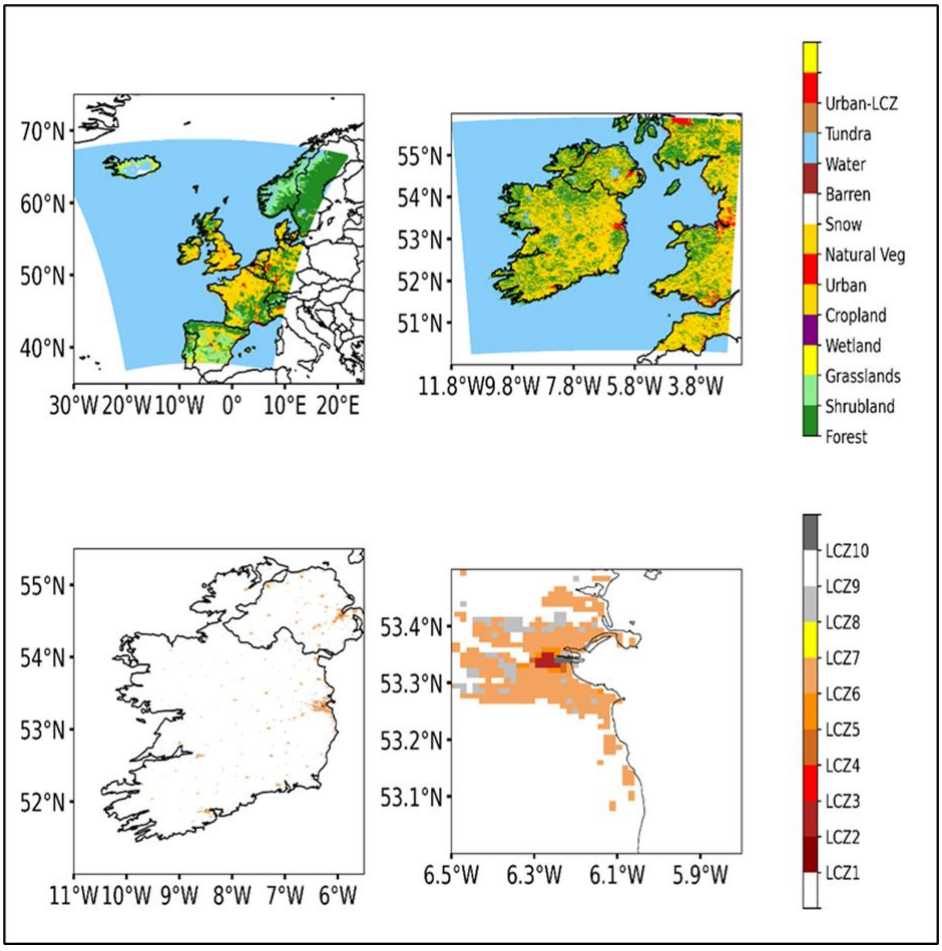

Figure B2: The outer domain at 10 km resolution, (b) our inner study region which covers the entire island of Ireland at 1 km resolution. Urban Climate Zones (UCZs) across (left) inner domain and (right) Dublin at 1 km resolution

At present the WRF modelling system has two default LULC classifications, based on either the United States Geological Survey (USGS), or the Moderate Resolution Imaging Spectro-radiometer (MODIS) information. The effect of changes in the LULC data on the local meteorology by comparing MODIS based and USGS-based dataset has been assessed in several parts of the world using WRF model. In our study we have used the Corine Land cover (CLC) which are distributed by the Copernicus Land Monitoring Service. Various studies have incorporated the update CORINE land use scheme across several parts of Europe and have seen improved model predictions in terms of various meteorological parameters (Buttner 2014; de -bode et al., 2023; de-Meij et al., 2022). We have utilized the 100-m spatial resolution CLC 2018 map in the WRF model as geographic static data. To adapt the CLC to the WRF, we followed Pineda et al. (2004) where they proposed the reclassification procedure of the 44 CLC categories into the

revised 21 Classes of MODIS LULC scheme. A WUDAPT-to-WRF python tool (Demuzere et al., 2022) was used to inject the LCZ information into WRF landuse tables. In the present study we have only replaced the urban areas within the CLC classification with the 10 urban climate zones (UCZ) in our study region.

Urban Canopy Modelling (UCM) is coupled with the WRF model to provide better representation of the physical processes involved in the exchange of heat, momentum, and water vapor in urban environment Currently, we are using the single layer UCM (SLUCM) in the present work over the urban areas. The SLUCM modelling considers the influence of street canyons, building parameters and estimates both the surface temperatures of, and heat fluxes from, three surface types: roof, wall, and road (Kusaka et al., 2001 WRF 4.3.1 incorporates the LCZs where MODIS and USGS tables have been extended from 33 to 41 classes and the WRF look-up tables have been modified to include the new urban classes. WRF also provides option of changing the heat capacity, thermal conductivity, surface albedo, surface emissivity and lower boundary temperature for roof, wall, and ground surface for all the LCZ categories. World Urban Database and Access Portal Tools (WUDAPT's, Ching et al., 2019) has created a global database for information of urban form and function of cities and captures variation across the urbanized landscape that includes the LCZ classification. Figure B2 shows the extent of UCZs in our inner domain and a close-up view is presented for the Dublin region. Most of the UCZ in Dublin can be categorised as LCZ 6 (Open low-rise), LCZ 4 (Open high-rise) and LCZ 2 (Compact midrise) especially in the city centre.

B.3.3 Initial and Boundary conditions

The initial and boundary conditions for the model are derived from ERA5 Reanalysis which is at 0.25° x 0.25° resolution (Hersbach et al., 2020). ERA5 is the fifth generation of ECMWF atmospheric reanalyses of the global climate, covering the period January 1950 to near real-time. ERA5 provides hourly estimates of a variety of atmospheric, land, and oceanic climate variables. The data covers the Earth on a ~30 km grid and resolves the atmosphere using 137 levels from the surface up to 0.01 hPa.

B.4 Parametrization schemes

An accurate representation of meteorological processes is important to accurately predict meteorology and air quality. There are several options provided in the model to parameterize cloud microphysics, the surface layer, land surface model (LSM), cumulus parameterization, atmospheric radiation, and planetary boundary layer (PBL). WRF offers multiple physics options which could be simple and efficient, more computationally costly, newly developed, or well-tried schemes in current operational models. The physical parameterization schemes used in the present study (Table B1) are the optimal combination of schemes used in various WRF based studies over Europe (Khan et al., 2019; Mar et al., 2016; Silveira et al., 2021).

A brief note on the role of each physical parameterization (Skamarock et al., 2021) and the scheme utilized in the current study is given below

Surface Layer: The main role of the surface layer schemes is to calculate friction velocities and exchange coefficients. These two variables are used by the land-surface models to calculate the surface heat and moisture fluxes by the planetary boundary layer scheme to estimate surface stress. Currently, each surface layer option is tied to a particular boundary-layer option. In the present study we utilize the revised Monin-Obukhov similarity theory (Jimenez et al., 2012). This scheme uses stability functions to compute surface exchange coefficients for heat, moisture, and momentum and is revised for stable and unstable conditions as well as the transition periods.

Table B1: Overview of the various option used to setup WRF

Domain	Double nested domain: ● Outer domain at 10 km resolution (252 × 345 grids) ● Inner domain at 1 km resolution (551 × 611 grids)
Land use and representation of urban areas	● Corine Land use dataset with default MODIS classification parameter ● Urban areas represented by built-up Local climate Zones (LCZs)
Meteorological initial and boundary conditions	ERA5 Reanalysis
Physical parameterization schemes	● Cloud microphysics : Lin et al. (1983) scheme, ● Convective Parameterization: The Grell-3D scheme based on Grell and Devenyi (2002), ● Microphysics : Morrison et al. (2008) scheme, ● Surface Layer Parameterization: Revised Monin-Obukhov similarity theory (Jimenez et al. 2012), ● Land Surface Model: Noah-MP land surface model (Chen and Dudhia 2001), ● Boundary Layer Parameterization: The Yonsei University PBL (Hong et al., 2006), ● Longwave and shortwave Radiation: Rapid Radiative Transfer Model (RRTMG, Iacono et al. (2008))

Planetary Boundary Layer: The planetary boundary layer (PBL) scheme is responsible for vertical sub-grid-scale fluxes due to eddy transports and in the whole atmospheric column. The Yonsei University PBL (Hong et al., 2006) has an explicit treatment of the entrainment layer at the PBL top and uses counter-gradient terms to represent fluxes due to non-local gradients. As compared to other PBL schemes, there are several improvements in the YSU PBL such as the analysis of interaction between the boundary layer and precipitation physics, topographic drag effects, top-down mixing, etc.

Land-Surface Model: The land-surface models (LSMs) use atmospheric information from the surface layer scheme, radiative forcing from the radiation scheme, and precipitation forcing from the microphysics and convective schemes, together with internal information on the land's state variables and land-surface properties, to provide heat and moisture fluxes over land and sea-ice points. The scheme provides sensible and latent heat fluxes to the boundary-layer scheme. At a later stage of current work, we would be focussing on the urban physics using the Urban Canopy Model which can be run as an option with the Noah and Noah-MP LSMs. Hence, we have fixed the NOAH LSM for our study. The Noah LSM is a widely used for research and operational purposes which advances the work by Chen and Dudhia (2001). This is a 4-layer soil temperature and moisture model with canopy moisture and snow cover prediction and includes root zone, evapotranspiration, soil drainage, and runoff, vegetation categories, monthly vegetation fraction, and soil texture.

Microphysics: This parameterization includes explicitly resolved water vapor, cloud, and precipitation processes. The various microphysics options have different numbers of moisture variables, depending on the ice-phase and mixed-phase processes included. The Morrison et al. (2008) scheme is based on the two-moment bulk microphysics and includes five species of hydrometeor: cloud droplets, cloud ice, rain, snow, and graupel/hail. The prediction of two-moments (i.e., both number and mass mixing ratio) allows for a more robust treatment of the particle size distributions, which are a key for calculating the microphysical process rates and cloud/precipitation evolution.

Cumulus Parameterization: These schemes estimate the sub-grid-scale effects of convective and/or shallow clouds and represent vertical fluxes due to unresolved updrafts, downdrafts, and compensating motion outside the clouds. Cumulus parameterizations are theoretically only valid for coarser grid sizes, (e.g., greater than 10 km), and should not be used when the model can resolve the deep convective updrafts itself (e.g., ≤ 4 km grid). As our inner domain is finely resolved at 1km, we only use the cumulus scheme for the outer domain at 10 km. The Grell-3D scheme is essentially improved version of Grell-Devenyi Ensemble Scheme (2002) in which effectively multiple cumulus schemes and variants are run within each grid box and then the results are averaged to give the feedback to the model.

Atmospheric Radiation: The radiation schemes deal with the radiative flux divergence and surface longwave and shortwave radiation for the ground heat budget. The longwave radiative flux from the ground is controlled by the surface emissivity which depends on land-use type, and skin temperature. Shortwave radiation includes visible and surrounding wavelengths that make up the solar spectrum and includes processes such as absorption, reflection, and scattering in the atmosphere and at surfaces. For shortwave radiation upward flux is the reflection due to surface albedo. The Rapid Radiative Transfer Model (RRTMG, Iacono et al. (2008)) is a state-of the-art model for weather and climate applications both globally and regionally.

B.4 Model Validation

For the model evaluation, the first 24 hours were taken for model spin-up in all the model runs while the model is evaluated for the remaining number of days. In addition, the model is only evaluated for the inner domain (d02: Ireland) for 2m air temperature,

There are several evaluation statistical methods that can be used to evaluate the performance of a model. However, there is no single statistical method that condenses all phases of interest. To provide a robust evaluation process, it is therefore important to consider different performance statistics and to understand the type of information they might provide. In this study, a few statistics of the model outputs are computed to find the optimal land use integration over Ireland.

Table B2: The statistical parameters used to evaluate model performance

Metrics	Formula	Range	Ideal Value	Benchmark
Mean Bias Error (MBE)	$\overline{x_{WRF} - x_{obs}}$	(-∞, ∞)	0	Wind speed= 0.5 m/s Temperature = 0.5 C
Root Mean Square Error (RMSE)	$\left(\overline{\lvert x_{WRF} - x_{obs}\rvert^2}\right)^{0.5}$	(0, ∞)	0	Wind speed= 2m/s Temperature= 2 C
Correlation	$\frac{\sum_i^n (x_{WRF} - \overline{x_{WRF}})(x_{obs} - \overline{x_{obs}})}{(\sum_1^n (x_{WRF} - \overline{x_{WRF}})^2)^{0.5} (\sum_1^n (x_{obs} - \overline{x_{obs}})^2)^{0.5}}$	(-1,1)	1	

where x_{WRF} represents the simulated parameter by WRF and x_{obs} is the observed parameter.

The various statistical framework is rooted in previous studies used where they have successfully (e.g Gbode et al., 2019; Sati and Mohan 2016; Thacker and Holler 2023). These statistical metrics used are summarised below while the formula are listed in Table B2

a. Correlation coefficient (r); The correlation coefficient measures of the strength of the linear relationship between model and observations.
b. The Root Mean Square Error (RMSE): RMSE is commonly used measure of the performance of model outputs with respect to observation. The RMSE tends to aggregate the magnitudes of the errors in predictions for various data points into a single measure of predictive power. RMSE are non-negative values whose scale depends on the scale of the dataset being compared. A RMSE of 0 represents a perfect relationship.
c. The Mean bias error (MBE) estimates the relative bias of model predictions.

Figure B3 shows the comparison of model simulated temperature and wind speed with observations at various met stations in Dublin. The comparison for wind speed is limited to just two stations as the values were not available at Pheonix Park. The model does well in stimulating the diurnal variation of both temperature and wind speed at the three stations. The model captures the afternoon high values and morning cooler temperatures. Similarly, the high and lows of wind speed are also captured by the model. There is a slight overestimation of temperature (<0.5 C) and wind speed (<1 m/s) during nighttime at Dublin Airport. The model simulated temperature shows slight underestimation of temperatures (<0.5 C) during some hours of the day at the three stations.

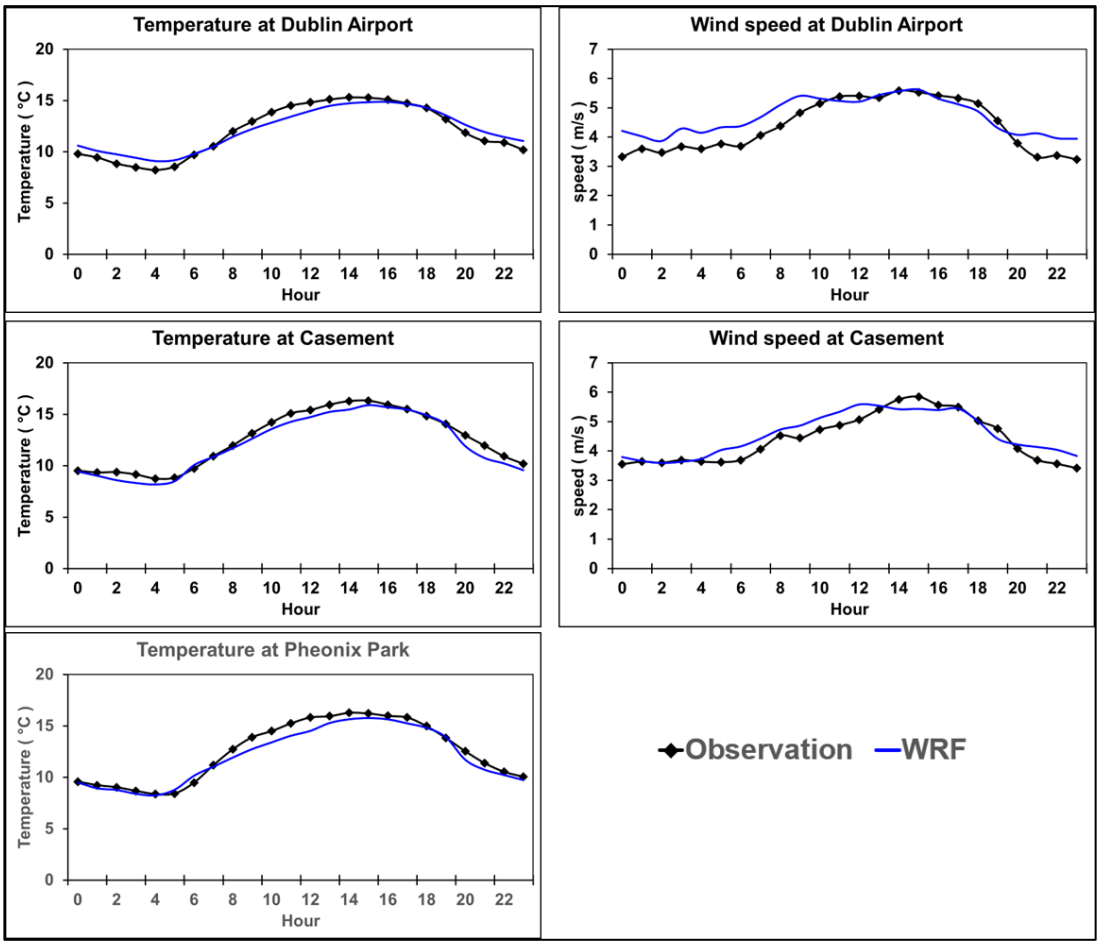

Figure B3: Comparison of Model simulated average diurnal temperature and wind speed with observations from Met Eireann Stations

The corresponding statistical evaluation of model performance is provided in Table B3. The correlation coefficient for both the variables is more than 0.90 at the stations and the RMSE values for temperature are around 1.5 °C and for wind 1.2 m/s which are well within the 2.0 °C and 2 m/s standard by WMO. Similarly, the MBE values for temperature and wind speed are below the 0.5 °C and 0.5 m/s WMO

benchmark. This model performance evaluation gives us the confidence of it performing well for our study region and simulation duration.

Table B3: Statistical evaluation of model simulated temperature and wind speed at various stations in Dublin

	Temperature			Wind speed		
	MBE (°C)	RMSE (°C)	r	MBE (m/s)	RMSE (m/s)	r
Dublin Airport	0.14	1.66	0.91	0.31	1.29	0.84
Casement	0.42	1.48	0.95	0.11	1.05	0.93
Pheonix Park	0.43	1.45	0.95			

References

Chen, F., and Dudhia J., (2001). Coupling an advanced land-surface/ hydrology model with the Penn State/ NCAR MM5 modeling system. Part I: Model description and implementation. Mon. Wea. Rev., 129, 569–585.

Chen, F., Kusaka, H., et al., (2011), The integrated WRF/urban modelling system: development, evaluation, and applications to urban environmental problems. Int. J. Climatol., 31: 273-288.

Grell, G. A., and D. Devenyi, 2002: A generalized approach to parameterizing convection combining ensemble and data assimilation techniques. Geophys. Res. Lett., 29(14), Article 1693.

Grell, G.A., Peckham, S.E., Schmitz, R., McKeen, S.A., Frost, G., Skamarock, W.C., Eder, B., 2005. Fully coupled "online" chemistry within the WRF model. Atmos. Environ. 39, 6957–6975. https://doi.org/10.1016/j.atmosenv.2005.04.027

Hersbach, H., Bell, B., Berrisford, P., Hirahara, S., Horányi, A., Muñoz-Sabater, J., Nicolas, J., Peubey, C., Radu, R., Schepers, et al. (2017): Complete ERA5 from 1979: Fifth generation of ECMWF atmospheric reanalyses of the global climate. Copernicus Climate Change Service (C3S) Data Store (CDS). Accessed 10.10.2021.

Hong, S.-Y., Noh, Y. and Dudhia J., (2006). "A new vertical diffusion package with an explicit treatment of entrainment processes." Mon. Wea. Rev., 134, 2318–2341.

Iacono, M. J., Delamere J. S., Mlawer E. J., Shephard M. W, Clough S. A., and Collins, W. D. (2008). "Radiative forcing by long-lived greenhouse gases: Calculations with the AER radiative transfer models." J. Geophys. Res., 113, D13103.

Ioannou, K., Karampatzakis, D., Amanatidis, P., Aggelopoulos, V., & Karmiris, I. (2021). Low-Cost Automatic Weather Stations in the Internet of Things. Information, 12(4), 146. https://doi.org/10.3390/info12040146

Jimenez, P., Dudhia J., Gonzalez-Ruoco J. F., Navarro J., Montavez J. P., and Garcia Bustamente E., (2012). "A revised scheme for the WRF surface layer formulation". Mon. Wea. Rev., 140, 898–918.

Jiménez-Esteve, B., Udina, M., Soler, M. R., Pepin, N., & Miró, J. R. (2018). Land use and topography influence in a complex terrain area: A high-resolution mesoscale modelling study over the Eastern Pyrenees using the WRF model. Atmospheric Research, 202(November 2017), 49–62. https://doi.org/10.1016/j.atmosres.2017.11.012

Brotzge, J. A., and Coauthors, 2023: Challenges and Opportunities in Numerical Weather Prediction. Bull. Amer. Meteor. Soc., 104, E698–E705, https://doi.org/10.1175/BAMS-D-22-0172.1.

Büttner, G. (2014). CORINE Land Cover and Land Cover Change Products BT - Land Use and Land Cover Mapping in Europe: Practices & Trends (I. Manakos & M. Braun (eds.); pp. 55–74). Springer Netherlands. https://doi.org/10.1007/978-94-007-7969-3_5

Ching, J., et al (2018). WUDAPT: An Urban Weather, Climate, and Environmental Modeling Infrastructure for the Anthropocene. Bulletin of the American Meteorological Society, 99(9), 1907–1924. https://doi.org/10.1175/BAMS-D-16-0236.1

Khan M.A.H, Clements J., Lowe D., McFiggans G., Percival C.J., Shallcross D.E. (2019). Investigating the behaviour of the CRI-MECH gas-phase chemistry scheme on a regional scale for different seasons using the WRF-Chem model. Atmospheric Research. 229:145-56.

Lin, Y.L., R. D. Farley, and H. D. Orville, 1983: Bulk parameterization of the snow field in a cloud model. J. Climate Appl. Meteor., 22, 1065–1092.

Mar K.A., Ojha N., Pozzer A., Butler T.M. Ozone air quality simulations with WRF-Chem (v3.5.1) over Europe: model evaluation and chemical mechanism comparison. Geoscientific Model Development. 2016;9(10):3699-728.

Michalakes, J., Dudhia J., Gill D., Henderson T., Klemp J., Skamarock W., and Wang W., (2004). "The Weather Research and Forecast Model: Software Architecture and Performance. To appear in proceeding of the Eleventh ECMWF Workshop on the Use of High-Performance Computing in Meteorology." 25–29 October 2004, Reading, U.K., Ed. George Mozdzynski.

Morrison, H., and Gettelman A., (2008). "A New Two-Moment Bulk Stratiform Cloud Microphysics Scheme in the Community Atmosphere Model, Version 3 (CAM3). Part I: Description and Numerical Tests." J. Clim. 21, 3642–3659.

Nolan, P. (2024). Research 471: Updated High-resolution Climate Projections for Ireland EPA Research Report

Sati A.P., and Mohan M. (2018). "The impact of Urbanization during half a century on surface meteorology based on WRF model simulations over National Capital Region, India." Theoretical and Applied Climatology.134: 309–323.DOI 10.1007/s00704-017-2275-6

Segura, R., Badia A., Ventura S., Gilabert J., Martilli A., and Villalba G. (2021). "Sensitivity study of PBL schemes and soil initialization using the WRF-BEP-BEM model over a Mediterranean coastal city." Urban Climate 39. DOI: 10.1016/j.uclim.2021.100982

Silveira C, Martins A, Gouveia S, Scotto M, Miranda AI, Monteiro A. The Role of the Atmospheric Aerosol in Weather Forecasts for the Iberian Peninsula: Investigating the Direct Effects Using the WRF-Chem Model. Atmosphere 2021. 12(2), 288; https://doi.org/10.3390/atmos12020288

Skamarock, W. C., Klemp, J. B., Dudhia, J., Gill, D. O., Liu, Z., Berner, J., … Huang, X. -yu. (2021). A Description of the Advanced Research WRF Model Version 4.3 (No. NCAR/TN-556+STR). doi:10.5065/1dfh-6p97

Thaker, J., & Höller, R. (2023). Evaluation of High Resolution WRF Solar. Energies, 16(8), 3518. https://doi.org/10.3390/en16083518

Vogel, J., & Afshari, A. (2020). Comparison of urban heat island intensity estimation methods using urbanized WRF in Berlin, Germany. Atmosphere, 11(12). https://doi.org/10.3390/atmos11121338

de Meij, A., Ojha, N., Singh, N., Singh, J., Poelman, D. R., & Pozzer, A. (2022). The Impact of High-Resolution SRTM Topography and Corine Land Cover on Lightning Calculations in WRF. Atmosphere, 13(7), 1050. https://doi.org/10.3390/atmos13071050

Demuzere, M. et al. (2022): A global map of local climate zones to support earth system modelling and urban-scale environmental science, Earth Syst. Sci. Data, 14, 3835–3873, https://doi.org/10.5194/essd-14-3835-2022

Gbode, I. E., Dudhia, J., Ogunjobi, K. O., & Ajayi, V. O. (2019). Sensitivity of different physics schemes in the WRF model during a West African monsoon regime. Theoretical and Applied Climatology, 136(1–2), 733–751. https://doi.org/10.1007/s00704-018-2538-x

Kusaka H., Kondo H., Kikegawa Y. and Kimura T. (2001). A Simple Single-Layer Urban Canopy Model for Atmospheric Models: Comparison with Multi-Layer and Slab Models. Boundary-Layer Meteorology, 101: 329–358

Pineda, N., Jorba, O., Jorge, J., and Baldasano, J. M. (2004). Using NOAA AVHRR and SPOT VGT data to estimate surface parameters: Application to a mesoscale meteorological model. International Journal of Remote Sensing, 25(1), 129–143. https://doi.org/10.1080/0143116031000115201

Powers, J. G., and Coauthors, 2017: The Weather Research and Forecasting Model: Overview, System Efforts, and Future Directions. Bull. Amer. Meteor. Soc., 98, 1717–1737, https://doi.org/10.1175/BAMS-D-15-00308.1.

Zhu J., and Ooka, R. (2023). WRF-based scenario experiment research on urban heat island: A review, Urban Climate, Volume 49, 101512, https://doi.org/10.1016/j.uclim.2023.

Appendix C: Explanation of Technical terms

Technical Term	Simplified Explanation
Urban Heat Island (UHI) effect	The phenomenon where cities are significantly warmer, especially at night, than the surrounding countryside. This is mainly because urban materials like asphalt and concrete absorb and trap more heat than natural landscapes, and tall buildings can block cooling winds. Furthermore, cities loose heat slower than the rural areas
Canopy-level and Surface UHIs	UHI is measured in two main ways: 1. Surface UHI refers to the temperature of the actual surfaces (like hot roads, roofs, and walls). The observations are typically from satellites 2. Canopy-level UHI refers to the warmer air temperature that people feel at street level, which directly impacts public health and comfort. The observations are from weather stations.
Local Climate Zones (LCZ)	LCZ framework classifies different types of urban landscapes (e.g., compact city centre, dense downtown, residential areas, industrial parks, etc). It allows city planners to understand precisely where and why the city gets hot, making adaptation strategies more targeted and effective.
Heating Degree Days (HDD) and Cooling Degree Days (CDD)	These are simple metrics that quantify the energy needed to heat or cool buildings. Cooling Degree Days measure how hot it is (reflecting the demand for air conditioning), and Heating Degree Days measure how cold it is (reflecting the demand for heating).
Lamb weather types (LWT)	The LWT scheme is a well-known synoptic classification of daily weather patterns developed by Hubert Lamb, that recognizes 27 types of flow and 7 main types of circulations viz., anticyclonic (A), cyclonic (C), northerly (N), easterly (E), southerly (S), westerly (W), north westerly (NW) and the unclassified type (U).
Anthropogenic heat emissions	This is simply waste heat released by human activities, such as heat escaping from cars, air conditioners, and industrial processes. This added heat contributes to the overall UHI effect.